Neural Selectivity and Representation of Gloss in the Monkey Inferior Temporal Cortex

Nishio Akiko

DOCTOR OF PHILOSOPHY

Department of Physiological Sciences

School of Life Science

The Graduate University for Advanced Studies

2011

Table of Contents

Abstract

Only from visual information, we can easily recognize whether an object is made of plastic or metal, or whether surface condition is slippery or not. How can we recognize material and surface condition of objects? Objects have specific surface reflectance properties that depend on the materials and fine structures of the surface. Surface gloss provides important information on the material composition of an object and the fine structure of its surface. Although gloss perception is very important for object recognition, little is known about the neural mechanisms related to gloss perception.

To study how gloss is represented in the visual cortical areas related to object recognition, I conducted single unit recording experiment to study neural selectivity and representation of gloss in the inferior temporal cortex of awake macaque monkeys performing a visual fixation task. In the first part of the experiment, I examined the relationship between neural responses and physical parameters related to gloss, and in the second part, I examined the relationship between neural responses and perceptual parameters related to gloss. In the first part of the experiment, I examined the responses of neurons to a set of object images having various combinations of specular reflection, diffuse reflection and roughness that are important physical parameters of surface gloss (gloss stimulus set). I found that there exist neurons in the lower bank of

the superior temporal sulcus in IT cortex that selectively responded to specific combination of surface reflectance parameters. I recorded the activities of 215 neurons that responded to the gloss stimulus set, and of these, 193 neurons exhibited selectivity to the gloss parameters.

However, I have to exclude the possibility that the selectivity is due to image features not particularly related to gloss. Images in the gloss stimulus set varied with respect to their local luminance pattern; that is, glossy stimuli have sharp light spots corresponding to highlights. It was therefore possible that these selective responses were due to the presence of a specific pattern of highlights in some stimuli. To test this possibility, I recorded the responses of the same neurons to the gloss stimulus set rendered on a different 3D shape and assessed whether the change in shape affected stimulus selectivity. In this manipulation, the local luminance pattern changed but perceived glossiness was maintained. Therefore, if the selectivity to gloss stimulus set is due to local image features, selectivity will change when 3D shape is changed. On the other hand, if the selectivity reflected the differences in the glossiness, selectivity will be maintained. Images in the gloss stimulus set also varied with respect to the mean chromaticity and luminance. It was therefore possible that the selectivity to gloss stimulus set was due to differences in the color and luminance of the stimuli. To test

this possibility, I tested the responses to stimuli in which the pixels were randomly rearranged within the object contour (shuffled stimuli). In this manipulation, average color and luminance were not changed but perceived glossiness was dramatically changed. Therefore, if the selectivity is due to the differences in the average color and luminance, selectivity will not change when the pixels are randomly rearranged. On the other hand, if the selectivity related to the glossiness, it should significantly change. I conducted these two sets of control experiments using stimuli with different shape as well as shuffled stimuli in 139 out of 193 neurons that exhibited selectivity to the gloss parameters. I defined neurons as gloss-selective (gloss-selective neurons) based on the following two criterions. The first criterion is that there was significant correlation between the response to the original shape and those to a different shape. The second criterion is that either the neuron did not show significant response to the shuffled stimuli (<10 spikes/s and/or $p > 0.05$, t-test) or the correlation between the patterns of stimulus selectivity obtained by stimuli with the original shape and the shuffled stimuli were not significant. Of the 139 neurons tested in these two control tests, 57 neurons satisfied both of these two criteria, and were regarded as gloss-selective neurons.

Illumination is another important factor involved in the image formation, and I have examined the effect of the change in illumination for 48 gloss-selective neurons.

When I compared the responses to the gloss stimulus set rendered under default natural illumination and those to the stimuli rendered under another natural illumination, 40 out of 48 gloss-selective neurons exhibited significant correlation between the two sets of responses. This result is consistent with the expectation that the selectivity of these neurons will be maintained because it has been shown that changing the illumination environment does not affect the apparent glossiness very much, as long as natural illumination is used, and confirms that gloss selectivity of gloss selective neurons is largely independent of a change in illumination.

The stimulus preference of gloss-selective neurons differed from cell to cell and, as a population, responses of gloss-selective neurons covered the entire region of the gloss space though there was a tendency for glossier stimuli to elicit stronger responses. In order to understand how different glosses are represented by the activities of population of gloss-selective neurons, I conducted multidimensional scaling (MDS) analysis using the neural distance between each stimulus pair. The results of MDS analysis showed that the population responses of gloss-selective neurons systematically represent a variety of gloss.

In the second part of the experiment, in order to understand how the responses of gloss selective neurons are related to perceived gloss, responses of gloss selective

neurons were mapped in perceptual gloss space in which glossiness changes uniformly. I found that responses of most gloss selective neurons could be explained by linear combinations of two parameters that are shown to be important for gloss perception. This result indicates that the responses of gloss-selective neurons and gloss perception are characterized by common parameters, and this suggests that the responses of gloss selective neurons are closely related to gloss perception. I conclude that in the visual cortex there exist some mechanisms to integrate local image features and extract information about surface gloss, and that this information is systematically represented in the IT cortex that plays an important role in object recognition.

Introduction

Objects have specific surface reflectance properties that depend on their material composition and the fine structures of their surfaces. Our visual system is able to extract information about these surface reflectance properties from the retinal image, and the resultant perception of surface quality plays an important role in the identification of materials and the recognition of objects (Hunter and Harold, 1987; Adelson, 2001; Maloney and Brainard, 2010). Attempts to understand the neural processing underlying the perception of surface qualities have emerged in recent years (Cant and Goodale, 2007; Arcizet et al., 2008; Koteles et al., 2008; Cavina-Pratesi et al., 2010; Hiramatsu et al., 2011), and functional imaging studies in human subjects have shown that the ventral higher visual areas are activated when subjects attend to or discriminate materials (Cant and Goodale, 2007; Cant et al., 2009; Cavina-Pratesi et al., 2010; Cant and Goodale, 2011).

In the present study, we used a set of stimuli with different reflection properties to examine how surface reflectance property is represented in the brain. An important component of surface reflectance is gloss, which strongly influences surface appearance and changes depending on the material composition and smoothness of a surface.

Therefore we concentrated on examining neural selectivity and representation of gloss. We first examined the relationship between neural responses and physical parameters related to gloss, and then we examined the relationship between neural responses and perceptual parameters related to gloss.

Physical parameters related to gloss

When incident light is reflected from surface, direction and strength of reflection are not always uniform. The reflectance properties such as direction and strength of reflection depend on the material composition and smoothness of the surface, and these differences in the directional distribution of the reflected light generate a variety of gloss. Spatial distribution of surface reflectance can be quantitatively expressed by the Bi-directional Reflectance Distribution Function (BRDF) that is a dataset describing the intensity of reflected light to a given direction resulting from a given direction of incident light. Because BRDF is a huge amount of dataset due to a combination of all direction of incident light and reflected light, many parametric models have been proposed to approximate real BRDF mainly for rendering computer graphics images. A key concept underling these parametric BRDF models is that surface reflection consists of two major components. One is specular reflection that is reflected in a direction with

the same angle but with an opposite direction from the incident light relative to the surface normal. The other component is diffuse reflection that is reflected uniformly across all the direction. In addition to these two major components, most parametric BRDF models also assume third component that represent microscopic unevenness of surface that spread the direction of the specular reflection. In this study, we used Ward-Duer model that is one of the parametric BRDF model in which BRDF is approximated by three refrectance parameters (specular reflectance indicating the strength of specular reflection, diffuse reflectance indicating the strength of diffuse reflection and roughness indicating the degree of microscopic unevenness of surface) that have been shown to be particularly important for characterizing surface gloss (Cook and Torrance, 1982; Ward, 1992; Ngan et al., 2005). With these three parameters, one can generate realistic computer graphics images of objects exhibiting a variety of surface glosses (Fig. 1A). In the present study, we manipulated these parameters to generate a set of visual stimuli and recorded the activities of single-units in the monkey visual cortex to explore neurons selective for surface gloss and to examine the response properties of these cells.

Perceptual parameters related to gloss

Although little study has been conducted to examine neural representation of gloss, a number of psychophygical studies have been done to characterize gloss perception and to understand visual features related to gloss (Beck and Prazdny, 1981; Hunter and Harold, 1987; Nishida and Shinya, 1998; Obein et al., 2004; Motoyoshi et al., 2007; Doerschner et al., 2010; Emrith et al., 2010). An earlier study of gloss perception was reported by Hunter (Hunter and Harold, 1987). He defined six visual phenomena related to perceived gloss: specular gloss, distinctiveness-of-image-gloss, haze, sheen, the absence-of-texture gloss, and contrast gloss. Beck and Prazdny showed importance of highlight to gloss perception, by manipulating highlight of object images (Beck and Prazdny, 1981). They reported that perceived gloss decay with increasing distance from highlight, and they concluded that gloss perception is a direct perceptual response to local visual cue, not due to inference of surface as reflecting light specularly. Importance of highlight in gloss perception has been supported by other studies (Hunter and Harold, 1987; Blake and Bulthoff, 1990; Berzhanskaya et al., 2005). Recently, importance of image-based information such as luminance statistics has been reported. Nishida and Shinya manipulated shape and gloss, and found that gloss perception is affected by changes in shape, and suggested that image-based information such as luminance statistics is important for gloss perception (Nishida and Shinya, 1998). More recently,

Motoyoshi et al reported importance of skewness of luminance histogram for gloss perception (Motoyoshi et al., 2007).

Ferwerda et al linked perceptual gloss to physical parameters of gloss (Ferwerda et al., 2001). To find important parameters for gloss perception, they asked subjects to judge the difference in gloss between pairs of objects and conducted MDS analysis using apparent gloss differences. They found that important dimensions for gloss judgment are 'Contrast gloss' and 'Distinctness of image gloss', and based on this result, they proposed perceptual gloss space (cd-space) consisting of c axis (Contrast gloss) and d axis (Distinctness of image gloss). In the cd-space, perceived gloss changes uniformly. c and d axes are useful parameters related to perceptual gloss, because one can manipulate perceived gloss uniformly by changing physical parameters. In the second part of the present study, in order to examine the relationship between perceived gloss and responses of gloss selective neurons, we conducted mapping of neuronal responses on the cd-space.

Previous physiological studies of material perception

Attempts to understand the neural processing underlying the perception of surface qualities have emerged in recent years (Cant and Goodale, 2007; Arcizet et al., 2008;

Koteles et al., 2008; Cavina-Pratesi et al., 2010; Hiramatsu et al., 2011). Cant and Goodale conducted functional imaging in human subjects using visual stimuli in which shapes and materials were combined (Cant and Goodale, 2007). They have shown that when subjects attend to materials, the ventral higher visual areas are activated. Hiramatsu et al. recorded neural responses using fMRI while the subject viewed various types of material images (Hiramatsu et al., 2011). They showed that responses in higher ventral visual area are more closely related to perceptual judgment, whereas responses in lower visual areas are more closely related to simple image features. These studies suggest that integration of simple image features takes place along the ventral visual pathway that finally generates neuronal representation of materials that correlate with our perception. In monkey visual cortex, there are only a few studies that examined responses of neurons related to material perception (Koteles et al., 2008; Arcizet et al., 2008). Both these studies examined coding of materials using images of real materials and visual stimuli had three-dimensional (3D) meso-structures specific to materials that generate complex fine pattern of shadings that depend on the materials. No previous study in monkey has examined about neural mechanisms of gloss perception.

Inferior temporal (IT) cortex: candidate area for coding gloss

It is well known that the inferior temporal (IT) cortex plays a key role in the visual recognition of objects. Neurons selectively responsive to complex patterns such as face, and those selective to texture and color have been shown to reside there (Bruce et al., 1981; Perrett et al., 1982; Desimone et al., 1984; Tanaka et al., 1991; Komatsu et al., 1992; Kobatake and Tanaka, 1994; Eifuku et al., 2004; Tsao et al., 2006; Conway et al., 2007; Yasuda et al., 2010). In addition, activities related to encoding the three-dimensional (3D) geometry of objects (Janssen et al., 2001; Yamane et al., 2008; Nelissen et al., 2009) as well as activities affected by illumination direction have also been recorded in the region within the superior temporal sulcus (STS) in the IT cortex (Vogels and Biederman, 2002; Komatsu et al., 2007; Koteles et al., 2008). Furthermore, a recent functional magnetic resonance imaging (fMRI) experiment using monkeys observed activities distinguishing glossy from matte surfaces in the STS (Okazawa et al., 2011). These results suggest that a variety of information closely related to encoding surface gloss converge in the STS, and that this is an ideal area in which to explore the activities of neurons conveying information about the surface gloss of objects. We found that neurons selectively responding to specific glosses are present in the STS, and that as a population these neurons systematically represent a wide range of glosses.

Materials & Methods

Surgery and recordings of neuron activities

We recorded neuron activities from three hemispheres of two monkeys (*Macaca fuscata* weighing 5.8 - 6.2 kg). Before starting the physiological experiment, a head holder and a recording chamber (rectangular in shape with an opening 10 mm or 15 mm × 10 mm at the edge) were surgically attached to the skull under aseptic conditions and general anesthesia (Fig. 2A). Neuron activities were recorded from the posterior bank of the STS in the central part of the IT cortex. The center of each recording chamber was located at 22 mm lateral and 8-10 mm anterior, based on the stereotaxic coordinates. Neurons were recorded extracellularly using tungsten microelectrodes (Frederick Hare) that were inserted vertically from the vertex. During the physiological recordings, we first mapped a wide region of the posterior bank of the STS, and assessed the visual responses to stimuli with a variety of glosses. The mapping region of each hemisphere is shown in Figure 2C. After mapping, guide tubes made of MRI compatible metal (titanium or gold) were inserted into the brain, targeting the regions where gloss-selective neurons were observed (Fig. 2B). We then sampled the neurons in these regions extensively. The tips of the guide tubes were positioned about 1 cm above the

targeted cortical regions. While the guide tubes remained inserted in the brain, we took MRI images to confirm the recording positions. All procedures for animal care and experimentation were in accordance with the U.S. National Institutes of Health *Guide for the Care and Use of Laboratory Animals* (1996) and were approved by our institutional animal experimentation committee.

Experimental apparatus and the task

During the experiments, the monkeys were seated in a primate chair and faced the screen of a CRT monitor (frame rate: 100 Hz, Totoku Electric) situated at a distance of 85 cm from the monkey. Eye position was monitored using an eye coil or an infrared eye camera system (ISCAN). Visual stimuli were generated using a graphics board (VSG, Cambridge Research Systems), then presented on the CRT monitor. Image resolution was 800 × 600 pixels (30 pixels/degree). Monkeys were required to fixate on a small white spot (visual angle: <0.1°) at the center of the display. A trial started with the presentation of the fixation spot, after which stimuli were presented five times within a trial. Each stimulus presentation lasted 300 ms. The first stimulus was presented 800 ms after the monkey started fixating, and was followed by four stimuli with 300-ms interstimulus intervals. Monkeys were rewarded with a drop of juice 300 ms after

turning off the last stimulus. Monkeys had to maintain eye position within a 2.6° × 2.6° window centered at the fixation point. If the eye deviated from the eye window, the trial was canceled, and an intertrial interval (ITI) started. The duration of the ITI was 1000 ms. When the stimulus was presented on the fovea, the fixation spot was turned off after the first 500 ms of presentation to avoid interference between the fixation spot and the visual stimulus.

Visual stimuli

In this study, we used physical parameters and perceptual parameters to define visual stimuli to examine neural selectivities. In the first part of the experiment, we examined the relationship between neural responses and physical parameters of gloss. To assess the selectivity for surface reflectance properties of neurons in the STS, we generated visual stimuli having 33 types of surface reflectance selected from MERL BRDF dataset (http://www.merl.com/brdf/)(Fig 1B). This dataset contains data for about 100 materials (Matusik et al., 2003), and we selected 33 surfaces with the aim of producing stimuli that were as dissimilar in appearance as possible. The surface reflection of many materials can be represented by a combination of two components (diffuse reflection and specular reflection), and the reflection properties can be

characterized by three parameters: diffuse reflectance (ρd), indicating the strength of the diffuse reflection; specular reflectance (ρs), indicating the strength of specular reflection; and roughness (α), indicating the fine scale unevenness of the surface that causes the spread of specular reflection (Fig 1A). Examples of the appearance changes caused by a change in each parameter are shown in Fig. 1A. An object with low ρd and ρs is a black matte object (left). As ρd increases, the object becomes lighter (upper middle). As ρs increases, the object becomes shiny with sharp highlights if α is small, or with blurred highlights if α is large. To render the stimuli, ρd and ρs were set for R, G and B separately because the color of the diffuse and specular reflections varied across surfaces. Roughness α did not depend on color. We thus controlled 7 parameters (ρd_r, ρd_g, ρd_b, ρs_r, ρs_g, ρs_b, α), and the values for the Ward-Duer model, one of the BRDF models given in Ngan et al. (Ngan et al., 2005), were employed. Figure 1E shows the distribution of the reflection parameters in 3D space, which will be referred to as gloss stimulus space. In this plot, ρd indicates the mean of ρd_r, ρd_g and ρd_b, while ρs indicates the mean of ρs_r, ρs_g and ρs_b. Glossy stimuli with strong highlights (large ρs and small α) are located to the back and left, shiny stimuli with blurred highlights (large ρs and large α) are located to the back and right, and matte stimuli (small ρs) are located to the front and right. Although this plot ignores the variation of ρd and ρs

across RGB channels, it can still capture essential features of gloss selective neural responses. This gloss stimulus space will be used often in this paper because it is useful for visualizing stimuli and the gloss-selective responses of neurons.

In the later part of the experiment, we examined the relationship between neural responses and perceptual parameters of gloss. For this experiment, we prepared visual stimuli in which c and d values were uniformly distributed on the cd-space (cd-space stimulus). d value corresponds to 1 - α, and c value is a non-linear combination of ρd and ρs, and is defined as follows:

$$c = \sqrt[3]{\rho_s + \rho_d / 2} - \sqrt[3]{\rho_d / 2}$$

The stimulus set consisted of 4 levels of c values (0.0625, 0.125, 0.1875, 0.25), and d values (d = 0.8002, 0.8668, 0.9334, 1) with 3 levels of ρd (ρd = 0, 0.1, 0.4). I prepared 7 colors by changing the ratio among r, g, b values ofρd (Gray, Red, Green, Blue, Magenta, Cyan, Yellow), and used the optimal color and shape for each neuron. Example of stimulus set is shown in Fig. 3 (ρd: 0.1, color: gray, shape: shape3).

We used LightWave software (NewTek) to generate ten different 3D shapes (Fig. 1C). For the illumination environment, we used one of the high dynamic range images from the Devebec dataset (http://ict.debevec.org/~debevec/)(Eucalyptus Grove; illumination #1) as the default. We rendered object images using Radiance software

(http://radsite.lbl.gov/radiance/), employing image parameters (surface reflectance, shape, illumination environment) as described above. Stimuli with shape 3 are shown in Fig. 1B, and examples of stimuli with other shapes are shown in Fig. 4. In a control experiment to examine the effect of illumination, we used another illumination environment image from the Devebec dataset (Campus at Sunset; illumination #2). The luminance values of the rendered images were linearly mapped to a low dynamic range using a mean value mapping method in which the mean value, including the background, was mapped to 0.5 and the pixels that exceeded 1 were clipped. The object images were then cut out at the object contour. The mean luminance of the objects ranged from 3.15 cd/m^2 to 78.2 cd/m^2, and the objects were presented on a gray background (10 cd/m^2). The objects subtended about 5 degrees of visual angle and were usually presented on the fovea. When the responses at the fovea was weak and stronger responses were evoked by the presentation of stimulus at a certain position out of fovea, stimulus selectivity was examined at that position (27 out of 215 neurons recorded, 6 out of 57 gloss-selective neurons, see Results section).

Test of gloss selectivity

The activities of single neurons were isolated through online monitoring during

the recording, as well as through offline spike sorting using a template matching algorithm. Offline analysis confirmed that all of the data reported in this paper were single neuron activities. When we isolated a single neuron, we conducted a preliminary test to assess its responsiveness to visual stimuli. For this test we employed a stimulus set consisting of 15 surface reflectance properties, including three sets of gloss parameters (large ρs and small α, large ρs and large α, zero ρs) combined with five colors/lightnesses (red, green, blue, white, black). We tested the neural responses using this preliminary gloss stimulus set with 10 object shapes, and when a neuron responded to at least one of the test stimuli, we determined the optimal shape for that neuron. In the subsequent main experiment, we examined gloss selectivity in detail using object images with the optimal shape and the 33 types of surface reflectance. In the early part of the experiment, we used only two (shapes 3 and 9) or 4 (shapes 2, 3, 9 and 10) shapes (16 of 57 gloss selective neurons described in Results). Neural responses were analyzed only for correct trials, and the minimum number of repetitions of each stimulus accepted for analysis was five. Mean firing rates were computed for a 300-ms period beginning 50 ms after stimulus onset. Baseline activities were computed for the 300 ms immediately prior to the onset of the first stimulus within a trial. Only neurons that showed a mean firing rate of more than 10 spikes/s and a significant increase in activity

in response to at least one stimulus ($p < 0.05$, t-test) were included in the sample of visually responsive neurons. The presence or lack of selectivity for the 33 types of gloss stimuli was examined using ANOVA, and the strength of the selectivity was quantified as a selectivity index that was defined as 1 - (minimum response)/(maximum response). With this selectivity index, as selectivity increases, the index value increases and will exceed unity if the minimum response is less than the baseline activity. The sharpness of the selectivity was quantified using two indices: the number of stimuli that elicited responses with amplitudes more than half that of the maximum response and a sparseness index defined as follows:

$$\text{sparseness index} = [1 - (\sum_{i=1,n} r_i / n)^2 / \sum_{i=1,n} (r_i^2 / n)] / (1 - 1 / \text{n})$$

where r_i is the firing rate to the ith stimulus in a set of n stimuli (Rolls and Tovee, 1995), (Vinje and Gallant, 2000). If r_i was a negative value, it was replaced to zero. The sparseness index indicates the degree to which responses are unevenly distributed across the set of stimuli. We used a modified version of the sparseness index (Vinje and Gallant, 2000) because we felt the result would be more intuitive if sharper selectivity yielded a larger index value. The sparseness index is at a minimum, with a

value of 0, when responses to all stimuli have the same magnitude. As the stimulus selectivity becomes sharper, the index becomes larger. If only one stimulus among the set evokes a response, the index is at a maximum and is equal to 1.

Examination of the effects of shape and illumination

To examine the effect of shape, we compared the responses to the gloss stimulus set across different object shapes. Responses were compared between the shape that yielded the strongest responses in the preliminary test (optimal shape) and that yielding the second-strongest responses (non-optimal shape) by computing correlation coefficient between two sets of responses. In addition, we conducted 2-way ANOVA with gloss and shape as factors to examine the main effect and their interaction.

To examine the effect of illumination, we compared the responses to the gloss stimulus set rendered with the optimal shape across different illuminations. Responses were compared between the default illumination (Eucalyptus Grove) and another illumination (Campus at Sunset) by computing correlation coefficient between two sets of responses. In addition, we conducted 2-way ANOVA with gloss and illumination as factors to examine the main effect and their interaction.

To examine the effect of shape and illumination, we also used a separability index

(Mazer et al., 2002) (Grunewald and Skoumbourdis, 2004); (Yamane et al., 2008); (Mysore et al., 2010) to quantify how well a neuron retained its selectivity for gloss across changes in shape or illumination. To compute the separability index for shape changes, we first tabulated the gross responses of each selective neuron in an $m \times n$ response matrix (M), where m and n corresponded to the different glosses and shapes, respectively. We then computed the singular value decomposition ($M = USV$) of the response matrix. If selectivity for gloss is independent of the shape, the responses are fully explained by the first principal components (*i.e.*, the product of the first columns of U and V); otherwise, the responses are explained by the second principal component to some extent. The separability index is defined as the squared correlation (r^2) between the actual responses and the predicted responses reconstructed from only the first principal components. We used a permutation test to determine whether a separability index was significantly larger than chance. We randomly permuted the mean neuronal responses for different glosses within each tested shape, and computed a separability index for the reshuffled responses. Permuting the responses within but not across shapes ensured that the mean permuted response averaged across glosses for a given shape would be the same as the mean observed response. Permutations were performed 1000 times. If the separability index value obtained experimentally exceeded the 95th

percentile of the distribution of the separability indices for the reshuffled responses, the neuron was deemed to have a separability index significantly larger than the chance level. We also assessed the extent to which the responses are explained by the second principal component obtained from the singular value decomposition. If the r^2 between the actual responses and the predicted responses computed from only the second columns exceeded the 95th percentile of the distribution of the r^2 for the reshuffled responses, the second principal component would be deemed to have made a significant contribution. The separability index for changes in illumination was computed in a similar manner.

Examination of the representation of gloss by the population of neurons

To better understand how gloss-selective neurons represent gloss, we conducted MDS analysis. First, Pearson's correlation coefficients (r) between the responses of the population of gloss-selective neurons to all possible stimulus pairs were computed, then nonclassical MDS (non-metric) was applied using 1-r as a distance, and the result was plotted on a 2-dimentional space. We also tested other distance metrics such as Euclidean distance or Spearman's correlation coefficient, but the results of the MDS analyses were similar, regardless of the distance metric used.

Results

Selective responses to a gloss stimulus set

In the first part of the experiment, I will describe the results obtained using stimuli based on the physical parameters of gloss. We examined neural responses to the gloss stimulus set consisting of 33 types of surface reflectance rendered with the optimal shape for each neuron. We found that there are neurons in the lower bank of STS that selectively respond to gloss. We recorded the activities of 215 neurons that responded to the gloss stimulus set. Of these, 193 neurons exhibited selectivity (ANOVA, $p < 0.05$).

Figure 5 shows responses of three representative neurons (Cells 1, 2 and 3) that exhibited selectivity for the gloss stimulus set. Cell 1 (Fig. 5A-C) strongly responded to stimuli with sharp highlights (*e.g.*, stimuli #8 and #13) and did not respond to stimuli with weak glossiness (*e.g.* stimuli #1 and #33). This neuron showed strong and sharp gloss selectivity (gloss selectivity index = 1.08, sparseness index = 0.51, see Experimental Procedures). Only six stimuli evoked more than a half-maximal response. Stimuli that induced strong responses in Cell 1 were clearly localized in gloss parameter space (Fig. 5C): strong responses were evoked by stimuli with large specular reflectance (ρs) and small roughness (α).

Cell 2 (Fig. 5D, E) selectively responded to shiny objects with blurred highlights; that is, objects with large specular reflectance and large roughness (*e.g.*, stimuli #21 and #24) (gloss selectivity index = 0.95, sparseness index = 0.46). Only three stimuli evoked more than a half-maximal response in this neuron.

Cell 3 (Fig. 5F, G) exhibited modestly sharp selectivity to gloss stimulus set broader than cells 1 and 2 (gloss selectivity index = 1.05, sparseness index = 0.32), with nine stimuli evoking more than a half-maximal response. This neuron strongly responded to matte stimuli without clear highlights and those with small specular reflectance and large roughness.

Effect of object shape and pixel shuffling within the stimulus

The results described above suggest there are neurons that selectively respond to images of objects with a specific gloss. However, images in the gloss stimulus set also varied with respect to their local luminance pattern; that is, glossy stimuli have sharp light spots corresponding to highlights whose patterns are roughly constant as long as the object shape and illumination environment are unchanged. It was therefore possible that the selective response of Cell 1 was due to the presence of a specific pattern of highlights in some stimuli. To test this possibility, we recorded the responses of the

same neurons to the gloss stimulus set rendered on a different 3D shape and assessed whether the change in shape affected stimulus selectivity. In Fig. 6A, the red line indicates the rank order of the responses of Cell 1 to the gloss stimulus set when the optimal shape (shape 3) was used. The blue line indicates the responses of the same neuron when a non-optimal shape (shape 2) was used and the responses were aligned according to the same stimulus order as the red line. This neuron exhibited significant main effects of both surface reflectance and object shape (2-way ANOVA, $p < 0.05$), as well as a significant interaction between the two. This means that there was some difference in the pattern of gloss selectivity between the two shapes. More importantly, however, the overall pattern of responses to shape 2 was similar to the pattern of responses to the optimal shape, and there was a clear tendency for the responses to gradually decline along the horizontal axis. Responses to the gloss stimulus set showed a strong correlation between the optimal and non-optimal shapes ($r = 0.86$), which significantly differed from zero ($p < 0.05$). These results indicate that even when the local luminance pattern was changed by changing the object shape, the gloss selectivity of this neuron was maintained; thus, stimulus selectivity does not appear to be due to the local luminance pattern.

Images in the gloss stimulus set also varied with respect to mean chromaticity and

luminance. To exclude the possibility that the response selectivity was due to differences in the color and luminance of the stimuli, we tested the responses to stimuli in which the pixels were randomly rearranged within the object contour (shuffled stimulus, Fig. 1D, Fig. 4B). In the shuffled stimuli, the luminance and color histograms of the pixels did not change, nor did the mean luminance and mean chromaticity, but the glossiness dramatically changed, particularly for the glossy stimuli. In Fig. 6A, the black line indicates the responses of Cell 1 to the shuffled stimuli aligned according to the same order as the red and blue lines. That Cell 1 did not show clear responses (maximum = 1.71 spikes/s) to the shuffled stimuli reveals that the selective responses to the original stimulus set was not due to the mean color or luminance of these stimuli. In Fig. 6B, responses of Cell 2 to images rendered on a non-optimal shape (shape 9) and to the shuffled stimuli are compared with the responses to the optimal shape. As with Cell 1, the pattern of selectivity for the gloss stimulus set was highly correlated between the optimal and non-optimal shapes (red and blue lines, $r = 0.82$, $p < 0.01$), and the responses to the shuffled stimuli were very weak (black line, maximum = 6.84 spikes/s).

The results were markedly different with Cell 3, however (Fig. 6C). With this neuron the responses to the gloss stimulus set were highly correlated between the optimal (shape 8) and non-optimal (shape 4) shapes (red and blue lines, $r = 0.87$, $p <$

0.01) but, unlike Cells 1 and 2, this neuron also strongly responded to the shuffled stimuli (black line, maximum = 25.6 spikes/s), and those responses also correlated with the responses to the optimal shape ($r = 0.71$, $p < 0.01$). This suggests that the activity of Cell 3 was strongly influenced by low-level image features such as the mean luminance and chromaticity.

From the neurons that exhibited sufficiently strong (>10 spikes/s) and selective responses to the gloss stimulus set (ANOVA, $p < 0.05$), we isolated neurons that were likely selective for glossiness by employing two criteria. First, a given cell should be responsive to a non-optimal shape, and the patterns of stimulus selectivity obtained with the optimal and non-optimal shapes should be significantly correlated ($p < 0.05$). Second, either the neuron does not show a significant response to the shuffled stimuli (<10 spikes/s and/or $p > 0.05$, t-test) or the correlation between the patterns of stimulus selectivity obtained with the optimal shape and shuffled stimuli are not significant. Neurons satisfying these two criteria were defined as "gloss-selective." Of the 194 neurons that exhibited selectivity for the gloss stimulus set in the optimal shape, we assessed the responses to more than one shape in 145, to the shuffled stimuli in 169 and to both in 139 neurons. The distribution of correlation coefficients obtained under each of these conditions is shown in Fig. 7. The abscissa represents the correlation coefficient

between the responses to the optimal shape and the shuffled stimuli, while the ordinate represents the correlation coefficient between the responses to the optimal and non-optimal shapes. The scatter plot includes neurons recorded in both tests (shape change and shuffling), whereas the histograms include neurons that were tested in only one of these tests (open bars). Many neurons (118/145, 81 %) exhibited significant correlation between the responses to the optimal and non-optimal shapes. With regard to the responses to the shuffled stimuli, 54 neurons (54/169, 32 %) did not show significant responses (left-most bar in the histogram). Of the remaining 115 neurons that showed clear responses, the correlation between the responses to the optimal shape and shuffled stimuli was not significant in 51 (51/115, 44%). Of 139 neurons tested under both control conditions, 57 satisfied the two criteria for gloss-selective neurons listed above (red circles in Fig. 7). Recording site of each of these 57 gloss-selective neurons is shown in Figure 2C. Gloss-selective neurons appeared localized within the range of IT cortex we have mapped. Cells 1 and 2 are examples of this group of neurons. On the other hand, 43 neurons showed significant correlation between the responses to the optimal and non-optimal shapes as well as between the responses to the optimal shape and shuffled stimuli (blue circles in Fig. 7). Cell 3 is an example of those neurons, which, presumably, selectively respond to the specific luminance or color of the stimuli.

We also examined the stability of the selectivity of 57 gloss-selective neurons employing the separability measure (Fig. 8). All neurons had a significant separability index, and most neurons showed separability index values greater than 0.7 (mean ± SD: 0.86 ± 0.08). In addition, only one neuron showed a significant r^2 computed using the second principal component. Taken together, these results confirm that gloss selectivity is largely independent of the change in stimulus shape. Most of the gloss-selective neurons showed strong selectivity for the gloss stimulus set, with a selectivity index larger than 0.6 (median = 1.02), and many also showed sharp selectivity, with a sparseness index larger than 0.3 (median = 0.43)(Fig. 9).

We next examined how the responses of gloss-selective neurons were affected by a change in object shape or by image shuffling at the population level by computing the rank order of the population responses in a way similar to what was done in Fig. 6. That is, we sorted the responses of each neuron to the non-optimal shape and shuffled stimuli according to the rank order of the responses to the optimal shape and then averaged the responses across the population (Fig. 10A). We found that responses to the non-optimal shape monotonically declined along the horizontal axis, which was similar to the pattern of responses to the optimal shape. By contrast, the responses to the shuffled stimuli were flat, indicating that little or no selectivity was retained after shuffling of

the image pixels. However, for neurons that showed clear responses to the shuffled stimuli (blue circles in Fig. 7), responses to both the non-optimal shape and shuffled stimuli showed similar monotonically decreasing patterns along the rank order of the optimal shape (Fig. 10B), indicating that the selectivity was maintained under both conditions. In the following, we will describe in more detail the response properties of the 57 neurons that satisfied both of the aforementioned criteria for gloss-selectivity.

Stimulus preference of gloss-selective neurons

The preferred stimulus of gloss-selective neurons differed from cell to cell. Figure 11 shows two other examples of gloss-selective neurons: one (Fig. 11A) responded selectively to stimuli with large specular reflectance (ρs), small roughness (α) and sharp highlights, while the other (Fig. 11B) responded selectively to stimuli with large roughness, regardless of the specular reflectance.

To examine how gloss-selective neurons responded as a population to the gloss stimulus set, we computed the population response to each stimulus. Figure 11E shows the normalized population average response to each stimulus. The population of gloss-selective neurons responded more or less to all of the stimuli, though there was significant variation in the response magnitudes across the stimulus set (ANOVA, $p <$

0.05). The ratio between the maximum and minimum of the normalized responses (to stimulus #13, 0.47 and to #33, 0.21, respectively) was 2.18, and there was a tendency for glossier stimuli to elicit stronger responses. This tendency was more clearly seen when the distribution of the preferred stimulus for each gloss-selective neuron was examined. Figure 11F depicts the number of neurons that showed a peak response to each stimulus in the gloss stimulus set. Peak responses frequently occurred with stimuli having large specular reflectance and little roughness, but occurred less frequently with stimuli having small specular reflectance. By contrast, neurons that maintained stimulus selectivity despite shape changes and image shuffling (neurons represented by the blue circles in Fig. 7) more often preferred stimuli with small specular reflectance or those with large roughness (Fig. 12).

Effects of the illumination environment

In all of the results described so far, object images were rendered under the same illumination environment (illumination #1, Eucalyptus Glove). Changing the illumination environment does not affect the apparent glossiness very much, as long as natural illumination is used (Fleming et al., 2003). Therefore, if the responses of gloss-selective neurons are related to encoding glossiness, we would expect that

selectivity for the gloss stimulus set would be retained, even after the illumination environment was changed. To test that idea, we assessed gloss selectivity of 48 of the 57 gloss-selective neurons using stimuli in which an object with the optimal shape was rendered under different illumination (illumination #2, Campus at Sunset, Fig. 1D, Fig. 4C). In Fig. 13A, the red line indicates the responses of Cell 1 to the optimal shape illuminated under illumination #1 (same as the red line in Fig. 6A), and blue line indicates the responses of the same neuron to the same stimulus set under illumination #2. The results are aligned according to the same order as the red line. We found that there was a clear tendency for the responses to gradually decline along the horizontal axis, and that the responses to the stimulus set under the two illumination conditions were highly correlated ($r = 0.81$, $p < 0.05$)(Fig. 13A, inset). Figure 13B summarizes the effect of the illumination condition (abscissa) and object shape (ordinate) on the activity of gloss-selective neurons tested under the two illumination conditions. Given our definition of gloss-selective neurons, all of these neurons showed significant correlation between their responses to the optimal and non-optimal shapes. Likewise, most of the neurons showed significant correlation between illuminations (40/48, 83.3%, red circles). This indicates that the gloss selectivity of these neurons was retained across different illuminations, which is consistent with the notion that apparent glossiness is rather

stable under different natural illumination conditions. Analysis based on the separability measure also showed that the selectivity of gloss-selective neurons is mostly stable under different illumination conditions (Fig. 14AB). All neurons but one showed significant separability index, and most neurons showed separability index values greater than 0.7 (mean ± SD: 0.84± 0.1). In addition, only two neurons showed a significant r^2 computed using the second principal component. These results confirm that gloss selectivity of these neurons is largely independent of a change in illumination.

To further examine how the population of gloss-selective neurons was affected by the illumination condition, the rank order of the responses obtained under illumination #2 was compared with that obtained under illumination #1 (Fig. 14C, red and blue lines, respectively). The average responses obtained under illumination #2 gradually decreased along the rank order of the responses obtained under illumination #1 (abscissa), indicating that selectivity was largely maintained at the population level.

Population encoding of gloss

How are different glosses encoded by the activities of gloss-selective neurons? Knowing which pairs of stimuli were differentiated and which pairs were not well

differentiated should provide a clue as to how different glosses are encoded by the population of gloss-selective neurons. To examine this problem, we computed a correlation coefficient (r) for the responses of the 57 gloss-selective neurons to all possible pairs of the 33 stimuli in the gloss stimulus set. Then (1 - r) was regarded as the neural distance between two stimuli and multidimensional scaling (MDS) analysis was applied to the resultant distance matrix, which contained the neural distances for all possible pairs of stimuli. Figure 15A and B depict the relationships between the responses of the 57 gloss-selective neurons for two example pairs of stimuli. Stimuli #3 and #8 (Fig. 15A) are quite different in color and luminance, but both have sharp highlights and similar glossiness. The population of gloss-selective neurons exhibited highly correlated responses to these two stimuli ($r = 0.92$), indicating that the neural distance between them was small. Stimuli #3 and #31 (Fig. 15B) are very different in appearance: stimulus #3 is highly glossy, whereas stimulus #31 is matte. The response patterns to these two stimuli were quite different, and the correlation between them was very weak ($r = 0.22$), indicating the neural distance was large. We computed the neural distances for all pairs of stimuli using the same procedure, after which the stimuli were arranged on a two-dimensional plane such that their relative positions on the plane maintained the neural distances as much as possible.

Figure 15C indicates the resulting diagram of this MDS analysis. The scree plot in Fig. 15C (inset) shows that two dimensions are sufficient to capture most of the variance of the neural distance (stress = 0.12) and to understand the basic aspects of the neural encoding of the stimulus set. In this diagram, stimulus pairs that yielded similar response patterns in the neural population are plotted near one another and those that yielded different response patterns are plotted farther away. At the left side of this figure, highly specular stimuli are accumulated. On the other hand, at the lower right glossy stimuli with blurred highlights are accumulated, and toward the upper right glossiness is reduced and matte stimuli are clustered at the top right. The results of the MDS analysis show that the population responses of gloss-selective neurons systematically represent a variety of glosses, and suggest that these neurons carry information that is closely associated with characterizing the surface gloss of objects.

Distribution of responses of gloss selective cells on the cd-space.

In the results described so far, we have used stimuli based on the physical parameters of gloss. In the following part, I will describe the results obtained using stimuli based on the perceptual gloss space. We examined the distribution of neural responses to the stimuli that uniformly distributed on the cd-space and with optimal shape and optimal

color for each neuron. We recorded neural responses of 48 of the 57 gloss-selective neurons to cd-stimulus set. Of these, 44 neurons exhibited significant response (>10 spikes/s and $p < 0.05$, t-test) and significant selectivity (ANOVA, $p < 0.05$) to cd-space stimulus set.

Fig. 16A shows responses of cell1 to cd-space stimulus set that strongly responded to stimuli with sharp highlights and did not respond to stimuli with weak glossiness (Fig.5A ~ C). Fig. 16B shows bubble plot of the responses of this neuron in the cd-space. Cell1 selectively responded to stimuli with large d values regardless of c values, and responses gradually changed along d axis. This result suggests that d (distinctness of image gloss) is an important parameter determining the responses of cell1. Middle and right panels in Fig. 16B show two other examples of gloss selective cells. Responses of cell2 gradually changed along c axis, and responses of cell3 gradually changed along intermediate direction between c and d axis. Although the direction in cd-space to which each neuron was most sensitive differed from cell to cell, responses of each example neurons appears to change linearly in the cd-space.

Multi-regression analysis of the responses in the cd-space.

To examine whether responses of gloss selective neurons can be adequately explained by linear combinations of c and d value, we computed predicted response by multi regression analysis using c and d. Fig. 17A shows the relationship between the actual responses and predicted responses of cell1 depicted in Fig 16A. Black circles indicate actual firing rates of cell 1, and magenta circles on the linear plane indicate predicted responses. Correlation coefficient between actual responses and predicted responses of this neuron were very high ($r=0.81$, $p < 0.05$). Most neurons tested showed similar results. Fig. 17B shows the distribution of correlation coefficient between actual responses and predicted responses of 44 gloss selective neurons. All but one neuron (43/44, 97%) showed significant correlation that differed from zero ($p < 0.05$). These data suggest that responses of most gloss selective neurons can be reasonably explained by a linear combination of c and d. These data indicate that stimulus parameters (c, d) that are important for perceived gloss are also very important parameters determining the responses of gloss selective neurons, suggesting that these neurons are closely associated with gloss perception.

Tuning direction

We examined tuning direction to which each gloss selective neuron was most sensitive

in cd-space. For each neuron, tuning direction was determined as the direction of the maximum slope of cd-regression plane. For example, if responses increase with increasing d or c, tuning direction is defined as either 0 degree and 90 degree, respectively. On the other hand, if responses increase with decreasing d or c, tuning direction is defined as either 180 degree and 270 degree, respectively (Fig. 18A). We computed tuning directions for 43 neurons that showed significant correlation between actual responses and predicted responses and the distribution of the tuning directions is shown in Fig. 18B. Tuning direction differed from cell to cell, and interestingly, tuning direction was not uniformly distributed. There appears cluster of cells tuned around 0 degree, and we did not find cells that were tuned between 270 degree to 330 degree.

DISCUSSION

Surface reflectance properties in object recognition

Information about the physical properties of an object, such as its hardness/softness, coldness/warmness and smoothness/roughness are very important for object recognition. In addition, information on the surface reflectance properties are tightly connected to the function of evaluating the biological significance of objects. For example, surface reflectance of foods significantly changes depending on whether the food is fresh or old, and that of animal body skin changes depending on the health conditions. We are very sensitive to such surface properties of both natural and man-made objects, and often our behavioral decisions are dependent upon them. This information is closely related to the optical and surface reflectance properties of an object, and understanding how these properties are represented in the brain is essential for understanding the neural mechanisms involved in object recognition.

Although many studies have been conducted with the aim of understanding the neural representation of object shape, color and texture (Bruce et al., 1981; Desimone et al., 1984; Tanaka et al., 1991; Komatsu et al., 1992; Kobatake and Tanaka, 1994; Op de Beeck et al., 2001; Freedman et al., 2003; Conway et al., 2007; Kiani et al., 2007;

Yamane et al., 2008), few attempts (Arcizet et al., 2008; Koteles et al., 2008) have been made to study the neural representation of surface reflectance properties, which are no less important than other visual attributes. In the present study, we found that there exist neurons in the lower bank of the STS that selectively respond to specific gloss. Gloss selectivity differed from cell to cell and MDS analysis revealed that as a population these neurons systematically represent a variety of gloss. These results provide strong evidence that IT cortex that plays an important role in object recognition is involved in processing information of gloss.

Comparison with previous studies

Two previous studies (Arcizet et al., 2008; Koteles et al., 2008) have examined selectivity of neurons to various materials having different surface reflectance properties. These studies have reported neurons selective for materials in either area V4 (Arcizet et al., 2008) and in the IT cortex (Koteles et al., 2008) and that these neurons exhibited invariance of material selectivity to the change in illumination direction to some extent. Both these studies have used visual stimuli consisting of various materials taken from CUReT BRDF dataset (http://www.cs.columbia.edu/CAVE/software/curet/).

Bidirectional-reflectance-distribution-function (BRDF) is one of the most general methods to quantitatively characterize surface reflectance properties, and CUReT BRDF dataset contains measured BRDF data of various materials (Dana et al., 1999). However, materials in this dataset generally have 3D meso-structure characteristic to each material that yields complex texture pattern of shading. Therefore, it is likely that neural activity selective for specific material is due to complex texture pattern of shadings that is specific to each material. On the other hand, objects sampled in MERL BRDF dataset employed in the present study do not have such 3D meso-structures, and we were able to study the neural selectivity to surface reflectance properties in isolation eliminating the influence of the shading texture patterns. Another merit of this dataset is that reflectance parameters (ρs, ρd, p0) of each material are provided (Ngan et al., 2005). We were able to systematically characterize neural selectivities to surface reflectance properties taking advantage of such merits of this dataset.

In the present study, we did not attempt to control the luminance and color of the stimuli within the stimulus set in the first part of the experiment. Rather, we intentionally picked up the stimuli to cover the entire range of MERL BRDF dataset such that as wide variety of surface reflectance properties of real objects can be tested to explore neurons sensitive to a variety of gloss. A drawback of such procedure is that we

cannot control the low level image statistics such as luminance and color. Therefore, we used shuffled stimuli to exclude selective responses due to such simple image features. In addition, in the second part of the experiment, we used stimulus set in which both color and luminance are controlled.

Classification of gloss-selective neurons

In the first part of the experiment, we employed two criteria to define gloss-selective neurons and identified 57 neurons that satisfied those criteria. This does not imply, however, that these neurons form a distinct group that can be clearly separated from other nearby neurons. As can be seen in Figure 7, red circles that represent gloss-selective neurons form a continuous distribution with other neurons, and there is the likelihood that some of those cells may also be involved in encoding gloss. In particular, the neurons represented by blue circles retained selectivity for the gloss stimulus set, even when the object shape was changed. Although these neurons may be responding to low-level image statistics, such as mean luminance or mean chromaticity, they may also be involved in encoding glossiness. Pixel shuffling causes large changes in the apparent gloss of specular stimuli, whereas the changes are small for matte stimuli. We think it is possible that the neurons represented by blue circles

selectively encode stimuli with low specularity, and the neuron depicted in Fig. 6C may be a good example. Nonetheless, in attempting to explore neurons selective for gloss, we opted to apply rather conservative criteria.

Invariance of gloss selectivity

The invariance of stimulus selectivity to changes in parameters such as position, size and contrast is a salient feature of IT neurons (DiCarlo and Cox, 2007), and the present study also showed that the gloss-selective responses of IT neurons exhibited a considerable degree of invariance to changes in stimulus shape and illumination. At the same time, however, the invariance was not complete. Incomplete invariance to the change in illumination is consistent with a previous study examining the selectivity to various materials (Koteles et al., 2008). What is the cause of such partial invariance and the shape- and illumination-dependence of the gloss selectivity? When we view an object, three factors, namely shape, surface reflectance and illumination environment, interact to form its retinal image and are thus intermingled within the image. Isolating each factor from the retinal image is a fundamental task of the visual system during the process of object recognition. One view posits that the visual system solves this inverse problem and isolates each factor (Xiao and Brainard, 2008; Anderson and Kim, 2009;

Kim and Anderson, 2010; Wijntjes and Pont, 2010), whereas another view posits that the visual system does not solve inverse problem and only imperfectly isolates each factor (Nishida and Shinya, 1998; Pont and te Pas, 2006; Motoyoshi et al., 2007; Sharan et al., 2008; Wendt et al., 2010). The partial invariance observed in the present study may indicate that these IT neurons are situated at an intermediate stage during the separation of factors or, alternatively, it may indicate that the visual system can only imperfectly separate each factor. Detailed comparison of the dependence of gloss perception on object shape with the dependence of the gloss selectivity of IT neurons on object shape may provide insight into the neural processes underlying perception during the separation of factors such as 3D shape and reflectance of objects.

Relationship with gloss perception

In the first part of the experiment, we examined gloss selectivity of neurons using stimuli defined by a combination of physical parameters of gloss (ρs, ρd, α). An important question is how the activities of these neurons are related to the gloss perception. Ferwerda et al has examined the relationship between these physical parameters of gloss and perceived gloss and derived a perceptually uniform gloss space (Ferwerda et al., 2001). Our present results of MDS analysis have shown that a variety

of gloss are systematically represented on a two-dimensional space, and it is observed that 'c' and 'd' systematically vary along orthogonal directions on this two dimensional plane obtained by MDS analysis (data not shown). Then we directly examined the relationship between neuronal responses and cd-space in the second part of the experiment. We found that responses of gloss selective neurons can be explained by linear combination of 'c' and 'd'. This suggests that the activities of the gloss selective neurons recorded from IT cortex may be closely associated with gloss perception. In this experiment, we observed that tuning directions in cd-space are not uniformly distributed (Fig. 18B). This may be related to some property of our gloss perception. For example, direction of 330 degree in cd-space is the direction in which highlight becomes sharper but at the same time becomes weaker. There is the possibility that such event is rare and ethologically this direction is not important for gloss perception. But this is an open question remained for future study.

Neural processes related to generating gloss selectivity

How is gloss selectivity in IT neurons generated from the neural processing in early visual areas? Detection of complex shapes is thought to be achieved through integration of local features such as local contrast, orientation, spatial frequency and

contour curvature (Riesenhuber and Poggio, 1999; Kourtzi and Connor, 2011). The visual features related to gloss perception are not yet well understood though the importance of highlights has been recognized for a long time (Beck and Prazdny, 1981; Hunter and Harold, 1987; Blake and Bulthoff, 1990; Berzhanskaya et al., 2005) and the importance of image statistics has been suggested more recently (Nishida and Shinya, 1998; Motoyoshi et al., 2007; Sharan et al., 2008). That the responses of the gloss-selective neurons in the present study were significantly diminished by shuffling of the image pixels indicates their selectivity is not due simply to low-level image statistics: a difference in the parameters of the luminance and chromaticity histograms of different stimuli, for example. How the responses of gloss-selective neurons are determined by the combination of image features will be an important question for future research and should enhance our understanding of the visual features involved in gloss perception.

Acknowledgements

I would like to express sincere gratitude to all people who helped me during my doctoral study. My deepest appreciation goes to Prof. H. Komatsu for his constant supervision, suggestion and constant encouragement through the doctoral program. I really thank him for teaching me the fun of research with his enthusiasm, his inspiration, and his great efforts to explain things clearly and simply. I am also deeply grateful to Dr. N. Goda for his inspiring suggestions and instructions about data analysis and technique of CG rendering.

I would also like to thank Dr. M. Ito for giving me constructive comments and suggestions for the study. Special thanks are also to Dr. K. Koida for comments and suggestion about programming and analysis technique. I would also like to extend my gratitude to all laboratory members. In particular, M. Togawa and M. Takagi greatly helped in establishing the experimental systems. All other members inspired me in research and life during the long hours in the laboratory.

Finally, I would like to express my gratitude to my parents and two brothers for their understanding and warm encouragement.

Reference

Adelson EH (2001) On seeing stuff: the perception of materials by humans and machines. Proc SPIE 4299:1-12.

Anderson BL, Kim J (2009) Image statistics do not explain the perception of gloss and lightness. J Vis 9:10.

Arcizet F, Jouffrais C, Girard P (2008) Natural textures classification in area V4 of the macaque monkey. Exp Brain Res 189:109-120.

Beck J, Prazdny S (1981) Highlights and the perception of glossiness. Percept Psychophys 30:407-410.

Berzhanskaya J, Swaminathan G, Beck J, Mingolla E (2005) Remote effects of highlights on gloss perception. Perception 34:565-575.

Blake A, Bulthoff H (1990) Does the brain know the physics of specular reflection? Nature 343:165-168.

Bruce C, Desimone R, Gross CG (1981) Visual properties of neurons in a polysensory area in superior temporal sulcus of the macaque. J Neurophysiol 46:369-384.

Cant JS, Goodale MA (2007) Attention to form or surface properties modulates different

regions of human occipitotemporal cortex. Cereb Cortex 17:713-731.

Cant JS, Goodale MA (2011) Scratching beneath the surface: new insights into the functional properties of the lateral occipital area and parahippocampal place area. J Neurosci 31:8248-8258.

Cant JS, Arnott SR, Goodale MA (2009) fMR-adaptation reveals separate processing regions for the perception of form and texture in the human ventral stream. Exp Brain Res 192:391-405.

Cavina-Pratesi C, Kentridge RW, Heywood CA, Milner AD (2010) Separate channels for processing form, texture, and color: evidence from FMRI adaptation and visual object agnosia. Cereb Cortex 20:2319-2332.

Conway BR, Moeller S, Tsao DY (2007) Specialized color modules in macaque extrastriate cortex. Neuron 56:560-573.

Cook RL, Torrance KE (1982) A reflectance model for computer graphics. ACM Trans Graph 1:7-24.

Desimone R, Albright TD, Gross CG, Bruce C (1984) Stimulus-selective properties of inferior temporal neurons in the macaque. J Neurosci 4:2051-2062.

DiCarlo JJ, Cox DD (2007) Untangling invariant object recognition. Trends Cogn Sci 11:333-341.

Doerschner K, Boyaci H, Maloney LT (2010) Estimating the glossiness transfer function induced by illumination change and testing its transitivity. J Vis 10:8 1-9.

Eifuku S, De Souza WC, Tamura R, Nishijo H, Ono T (2004) Neuronal correlates of face identification in the monkey anterior temporal cortical areas. J Neurophysiol 91:358-371.

Emrith K, Chantler MJ, Green PR, Maloney LT, Clarke AD (2010) Measuring perceived differences in surface texture due to changes in higher order statistics. J Opt Soc Am A Opt Image Sci Vis 27:1232-1244.

Ferwerda J, Pellacini F, Greenberg D (2001) A psychophysically-based model of surface gloss perception. In, pp 291-301: Citeseer.

Fleming RW, Dror RO, Adelson EH (2003) Real-world illumination and the perception of surface reflectance properties. J Vis 3:347-368.

Freedman DJ, Riesenhuber M, Poggio T, Miller EK (2003) A comparison of primate prefrontal and inferior temporal cortices during visual categorization. J Neurosci 23:5235-5246.

Grunewald A, Skoumbourdis EK (2004) The integration of multiple stimulus features by V1 neurons. J Neurosci 24:9185-9194.

Hiramatsu C, Goda N, Komatsu H (2011) Transformation from image-based to perceptual

representation of materials along the human ventral visual pathway. Neuroimage 57:482-494.

Hunter RS, Harold RW (1987) The measurement of appearance. Hoboken, Jersey, USA: John Wiley & Sons.

Janssen P, Vogels R, Liu Y, Orban GA (2001) Macaque inferior temporal neurons are selective for three-dimensional boundaries and surfaces. J Neurosci 21:9419-9429.

Kiani R, Esteky H, Mirpour K, Tanaka K (2007) Object category structure in response patterns of neuronal population in monkey inferior temporal cortex. J Neurophysiol 97:4296-4309.

Kim J, Anderson BL (2010) Image statistics and the perception of surface gloss and lightness. J Vis 10:3.

Kobatake E, Tanaka K (1994) Neuronal selectivities to complex object features in the ventral visual pathway of the macaque cerebral cortex. J Neurophysiol 71:856-867

Komatsu H, Ideura Y, Kaji S, Yamane S (1992) Color selectivity of neurons in the inferior temporal cortex of the awake macaque monkey. J Neurosci 12:408-424.

Komatsu H, Yasuda M, Goda N, Banno T (2007) Neural responses selective for the orientation of the luminance gradient in the inferior temporal cortex of the monkey. Neurosci Res 58:S36.

Koteles K, De Maziere PA, Van Hulle M, Orban GA, Vogels R (2008) Coding of images of materials by macaque inferior temporal cortical neurons. Eur J Neurosci 27:466-482.

Kourtzi Z, Connor CE (2011) Neural representations for object perception: structure, category, and adaptive coding. Annu Rev Neurosci 34:45-67.

Maloney LT, Brainard DH (2010) Color and material perception: achievements and challenges. J Vis 10:19

Matusik W, Pfister H, Brand M, McMillan L (2003) A data-driven reflectance model. ACM Trans Graph 22:759-769.

Mazer JA, Vinje WE, McDermott J, Schiller PH, Gallant JL (2002) Spatial frequency and orientation tuning dynamics in area V1. Proc Natl Acad Sci U S A 99:1645-1650.

Motoyoshi I, Nishida S, Sharan L, Adelson EH (2007) Image statistics and the perception of surface qualities. Nature 447:206-209.

Mysore SG, Vogels R, Raiguel SE, Todd JT, Orban GA (2010) The selectivity of neurons in the macaque fundus of the superior temporal area for three-dimensional structure from motion. J Neurosci 30:15491-15508.

Nelissen K, Joly O, Durand JB, Todd JT, Vanduffel W, Orban GA (2009) The extraction of depth structure from shading and texture in the macaque brain. PLoS One 4:e8306.

Ngan A, Durand F, Matusik W (2005) Experimental analysis of BRDF models. Pro Eurograp Symp Rendering 2:117-226.

Nishida S, Shinya M (1998) Use of image-based information in judgments of surface-reflectance properties. J Opt Soc Am A 15:2951-2965.

Obein G, Knoblauch K, Vienot F (2004) Difference scaling of gloss: nonlinearity, binocularity, and constancy. J Vis 4:711-720.

Okazawa G, Goda N, Komatsu H (2011) Cortical regions activated by surface gloss in the macaque visual cortex localized using fMRI. Program No. 485.16. In: Society for Neuroscience 41st Annual Meeting. Washington DC.

Op de Beeck H, Wagemans J, Vogels R (2001) Inferotemporal neurons represent low-dimensional configurations of parameterized shapes. Nat Neurosci 4:1244-1252.

Perrett DI, Rolls ET, Caan W (1982) Visual neurones responsive to faces in the monkey temporal cortex. Exp Brain Res 47:329-342.

Pont SC, te Pas SF (2006) Material-illumination ambiguities and the perception of solid objects. Perception 35:1331-1350.

Riesenhuber M, Poggio T (1999) Hierarchical models of object recognition in cortex. Nat Neurosci 2:1019-1025.

Rolls ET, Tovee MJ (1995) Sparseness of the neuronal representation of stimuli in the

primate temporal visual cortex. J Neurophysiol 73:713-726.

Sharan L, Li Y, Motoyoshi I, Nishida S, Adelson EH (2008) Image statistics for surface reflectance perception. J Opt Soc Am A Opt Image Sci Vis 25:846-865.

Tanaka K, Saito H, Fukada Y, Moriya M (1991) Coding visual images of objects in the inferotemporal cortex of the macaque monkey. J Neurophysiol 66:170-189

Tsao DY, Freiwald WA, Tootell RB, Livingstone MS (2006) A cortical region consisting entirely of face-selective cells. Science 311:670-674.

Vinje WE, Gallant JL (2000) Sparse coding and decorrelation in primary visual cortex during natural vision. Science 287:1273-1276.

Vogels R, Biederman I (2002) Effects of illumination intensity and direction on object coding in macaque inferior temporal cortex. Cereb Cortex 12:756-766.

Ward G (1992) Measuring and modeling anisotropic reflection. ACM SIGGRAPH Computer Graphics:265-272.

Wendt G, Faul F, Ekroll V, Mausfeld R (2010) Disparity, motion, and color information improve gloss constancy performance. J Vis 10:7.

Wijntjes MW, Pont SC (2010) Illusory gloss on Lambertian surfaces. J Vis 10:13.

Xiao B, Brainard DH (2008) Surface gloss and color perception of 3D objects. Vis Neurosci 25:371-385.

Yamane Y, Carlson ET, Bowman KC, Wang Z, Connor CE (2008) A neural code for three-dimensional object shape in macaque inferotemporal cortex. Nat Neurosci 11:1352-1360.

Yasuda M, Banno T, Komatsu H (2010) Color selectivity of neurons in the posterior inferior temporal cortex of the macaque monkey. Cereb Cortex 20:1630.

FIGURE LEGENDS

Figure 1. Gloss parameters and stimuli for assessing gloss selectivity

(**A**) Schematic illustration of three reflection parameters, diffuse reflectance (ρd), specular reflectance (ρs) and roughness (α). When ρd increases, the lightness of the object increases. When ρs increases, the highlights become stronger. When α increases, the highlights become blurred. (**B**) Example of a gloss stimulus set. The stimuli exhibit 33 types of surface reflectance selected from the MERL BRDF dataset and rendered on one of the shapes (shape 3) under default illumination (Eucalyptus Grove). Stimuli were ordered according to the magnitude of α. (**C**) Ten object shapes used for the experiment rendered with surface #8 in **B**. See **Fig. 4A** for examples with other surface reflectance properties. (**D**) top: Example of a shuffled stimulus generated by randomizing the pixels within the contour. bottom: Example of a stimulus rendered under different illumination (Campus at Sunset). See **Fig. 4B** and **4C** for examples with other surfaces. (**E**) Distribution of reflection parameters in a 3D space (gloss stimulus space). Numbers correspond to those in **B**.

Figure 2. Recording site

(A) Schematic image of one hemisphere and recording site. Red region indicates recording site. Recording site is in the lower bank of STS. (B) Image of structural MRI of monkey 1 with guide tube. Vertical black line indicates guide tube inserted at 22 mm lateral and 9 mm anterior in the stereotaxic coordinates. (C) Recording site of gloss-selective neurons are plotted on the flatted map of the lower bank of STS. Contours indicate regions where neuronal responses were examined in each hemisphere and different color represent different hemisphere. Map of 3 hemispheres are superimposed based on the stereotaxic coordinates. Each circle indicates the position where a gloss selective neuron was recorded. Blue, red and green correspond to left hemisphere of monkey1, right hemisphere of monkey1 and left hemisphere of monkey2, respectively.

Figure 3. Examples of cd-space stimulus.

Examples of stimulus set to examine the relationship between neural responses and perceptual gloss space. The stimulus set includes exhibit 16 types of surface reflectances that distribute in cd-space uniformly. The images are rendered on one of the shapes (shape 3) under default illumination (Eucalyptus Grove).

Figure 4. Examples of stimuli based on physical parameters.

(**A**) Examples of stimuli with ten different shapes and five different surface reflectances rendered under default illumination (Eucalyptus Glove). (**B**) Examples of shuffled stimuli (shape 3) with five different surface reflectances. (**C**) Examples of stimuli (shape 3) with five different surface reflectances rendered under illumination #2 (Campus at Sunset).

Figure 5. Responses to gloss stimulus set

(**A**) Responses of an example neuron (Cell 1) to the gloss stimulus set. The responses are depicted as raster plots and post-stimulus time histograms (PSTHs). Horizontal bars under the PSTHs indicate the stimulus presentation period. (**B**) Response magnitude of Cell 1 to each stimulus in the gloss stimulus set represented by the size of the object image. This neuron strongly responded to stimuli with sharp highlights and did not respond to stimuli with weak glossiness. (**C**) Response magnitude of Cell 1 to each stimulus in the gloss stimulus set represented as the diameter of a circle and plotted at the corresponding position in the gloss stimulus space. (**D**, **E**) Responses of another neuron (Cell 2) plotted using the same format as in **B** and **C**, respectively. This neuron selectively responded to shiny objects with blurred highlights due to large specular reflectance and roughness. (**F**, **G**) Responses of a third neuron (Cell 3) plotted using the

same format as in **B** and **C**, respectively. This neuron strongly responded to matte stimuli without clear highlights and to those with small specular reflectance and large roughness.

Figure 6. Effects of a change in object shape and pixel shuffling on the activity of the neurons depicted in **Fig. 5.**

(**A**) Responses of Cell 1 (the same neuron depicted in **Fig. 5A-C**) sorted according to the rank order of its response magnitude when the optimal shape was used. The horizontal axis indicates rank order for the optimal shape (shape 3); the vertical axis indicates response magnitude (with s.e.m). The red line depicts the responses to the optimal shape, the blue line those to the non-optimal shape (shape 2), and the black line those to the shuffled stimuli. Object images with the optimal shape are shown at the top in rank order. The inset shows the relationship between the responses to each stimulus in the gloss stimulus set for the optimal (horizontal axis) and non-optimal (vertical axis) shapes. (**B, C**) Responses of Cells 2 and 3, respectively. The optimal and non-optimal shapes were shapes 3 and 9 for Cell 2 and shapes 8 and 4 for Cell 3. The conventions are as in **A**.

Figure 7. Effects of shape change and pixel shuffling: population analysis

Horizontal axis indicates correlation coefficient between the responses to the optimal and non-optimal shapes, and vertical axis that between the responses to the optimal shape and shuffled stimuli. If a neuron did not exhibit significant response to the non-optimal shape or shuffled stimuli, they are plotted on the horizontal or vertical axis, respectively. We defined "gloss-selective" neurons using two criteria: 1) They should be responsive to a non-optimal shape, and there should be significant correlation between the patterns of stimulus selectivity between the optimal and non-optimal shapes ($p < 0.05$). And 2) they should not show significant response to shuffled stimuli (< 10 spikes/s and/or $p > 0.05$, t-test), or the correlation for the stimulus selectivity between the optimal shape and shuffled stimuli should not be significant. Red circles represent gloss-selective neurons that satisfied these two criteria. Blue circles represent cells that exhibited significant correlation between the responses to the optimal and non-optimal shapes, as well as between the responses to the optimal shape and shuffled stimuli. The histogram at the top depicts the distribution of the correlation coefficients between the responses to the optimal shape and shuffled stimuli. The histogram at the right depicts the distribution of correlation coefficients between the responses to the optimal and non-optimal shapes. In the histograms, the solid bars represent cells in which both

correlation coefficients were obtained, and the open bars represent cells in which only one of the correlation coefficients was obtained.

Figure8. Separability index for a change in shape.

(**A**) Distribution of the separability index for a change in object shape. The horizontal axis indicates the separability index, the vertical axis the number of cells. Filled and open bars respectively indicate significant and non-significant cells, based on the permutation test. (**B**) Distribution of r^2 between the actual and predicted responses computed from only the second principal component. Other conventions are the same as in (**A**).

Figure 9. Distribution of the selectivity and sparseness indices among gloss-selective neurons.

(**A**) Distribution of the selectivity indices of 57 gloss-selective neurons. The horizontal axis indicates the selectivity index, and the height of each bar indicates the number of cells (left vertical axis). Black lines indicate the cumulative percentage of indices (right vertical axis). The rightmost bar indicates cells with a selectivity index over 1.2. (**B**) Distribution of the sparseness indices of the 57 gloss-selective neurons. The horizontal

axis indicates the sparseness index. Other conventions are the same as in (**A**).

Figure 10. Rank order of the responses to the gloss stimulus set: population average

(**A**) Average of the responses of 57 gloss-selective neurons (red circles in **Fig. 7**) to stimuli with the optimal shape (red line), a non-optimal shape (blue line) and shuffled stimuli (black line), sorted according to the rank order of the responses to the optimal shape for each neuron. (**B**) Average of the responses of 43 neurons that showed significant correlation between the responses to the optimal shape and shuffled stimuli (blue circles in **Fig. 7**). Other conventions are the same as in **A**.

Figure 11. Stimulus preference of gloss-selective neurons

(**A, C**) Responses of a gloss-selective neuron that was selectively responsive to shiny objects with clear highlights (Cell 4). (**B, D**) Responses of another gloss-selective neuron that was selectively responsive to matte objects (Cell 5). Conventions are the same as in **Fig. 5B**, **C**. (**E**) Population average of the normalized responses of 57 gloss-selective neurons to each stimulus in the gloss stimulus set. (**F**) Numbers of gloss-selective neurons that showed a peak response to each stimulus in the gloss stimulus set.

Figure 12. Summary of the responses of neurons that showed a significant correlation in their responses between the optimal shape and shuffled stimuli. (**A**) Population average of the normalized responses of 43 neurons that showed a significant correlation between the responses to the optimal shape and shuffled stimuli (blue circles in Fig. 7) for each stimulus in the gloss stimulus set. (**B**) Number of neurons that showed a peak response to each stimulus in the gloss stimulus set.

Figure 13. Effects of illumination change

(**A**) Responses of Cell 1 (the neuron depicted in **Fig. 5A-C**) sorted according to the rank order of the response magnitudes under the default illumination (illumination #1, Eucalyptus Grove). The horizontal axis indicates the rank order of the responses, and the vertical axis indicates the response magnitude (with s.e.m.). The red line depicts the responses under illumination #1; the blue line depicts those under different illumination (illumination #2, Campus at Sunset). Object images rendered with illumination #1 are shown at the top. The inset shows the relationship between the responses to each stimulus in the gloss stimulus set under illuminations #1 (horizontal axis) and #2 (vertical axis). (**B**) Summary of the effects of the illumination and shape in 48 gloss-selective neurons tested under both illuminations. The horizontal axis

indicates the correlation coefficient between the responses under the two different illumination conditions, and the vertical axis indicates the correlation coefficient between the responses to the optimal and non-optimal shapes. Given our definition of gloss-selective neurons, all of these neurons showed significant correlation between their responses to the optimal and non-optimal shapes. Red circles represent neurons that showed significant correlation between the responses elicited under the two illumination conditions. The histogram at the top depicts the distribution of the correlation coefficients between the responses under the two illumination conditions. Solid bars represent neurons that exhibited significant correlation. The histogram at the right depicts the distribution of correlation coefficients between the responses to the optimal and non-optimal shapes.

Figure 14. Effect of illumination on responses among gloss-selective neurons.

(A) Distribution of separability indices for the change in illumination. Filled and open bars respectively indicate significant and non-significant cells, based on the permutation test. **(B)** Distribution of r^2 between the actual and predicted responses computed from only the second principal component. **(C)** Average of the responses of 57 gloss-selective neurons to stimuli with the optimal shape rendered under default

illumination (illumination #1, Eucalyptus Grove, red line) and another illumination (illumination #2, Campus at Sunset, blue line) sorted according to the rank order of the responses under illumination #1.

Figure 15. Neural representation of gloss in the activities of gloss-selective neurons

(**A**) Relationship between the responses of 57 gloss-selective neurons to a pair of stimuli (surface #3 and #8) that are similarly glossy in appearance. The horizontal axis indicates responses to one stimulus (#3), the vertical axis the responses to the other (#8).

(**B**) Relationship between the responses of 57 gloss-selective neurons to a pair of stimuli (surface #3 and #31) that differ with respect to their glossiness. Conventions are as in **A**.

(**C**) Two-dimensional plot of the results of non-classical MDS analysis. Distances were based on 1-r between the responses of the 57 gloss-selective neurons for each stimulus pair from the gloss stimulus set. The inset is a scree plot showing the relationship between the number of dimensions and the stress in the MDS analysis.

Figure 16. Responses to cd-space stimulus set

(**A**) Responses of an example neuron (Cell 1) to the cd-space stimulus set. The responses are depicted as raster plots and post-stimulus time histograms (PSTHs). Horizontal

bars under the PSTHs indicate the stimulus presentation period. (**B**) Response magnitude of Cell 1 (left), Cell 2 (middle) and Cell 3 (right) to each stimulus in the cd-space stimulus set represented as the diameter of a circle and plotted at the corresponding position in the cd-space.

Figure 17. Multi regression analysis

(**A**) Both actual response of Cell1 and predicted responses by multi regression analysis are plotted at the corresponding position in the three dimensional space consisting of c axis, d axis and firing rate (FR). Black circles indicate actual firing rates of cell 1, and magenta circles on the linear plane indicate predicted responses. There is significant correlation between actual responses of cell1 and predicted responses ($r=0.81$).

(**B**) Distribution of the correlation coefficient of the 44 gloss-selective neurons between the actual responses and predicted responses. The horizontal axis indicates the correlation coefficient. The height of each bar indicates the number of cells (left vertical axis). Filled and open bars respectively indicate cells exhibiting significant and non-significant correlation.

Figure 18. Tuning direction

(A) Definition of tuning direction is illustrated. If responses changed along d axis, tuning direction is defined as either 0degree or 180 degree. If responses changed along c axis, tuning direction is defined as either 90 degree or 270 degree.

(B) Distribution of the tuning directions of 43 gloss-selective neurons. One cell that showed non-significant correlation between actual responses and predicted responses by multi regression is excluded in this figure. Each blue arrow indicates one cell.

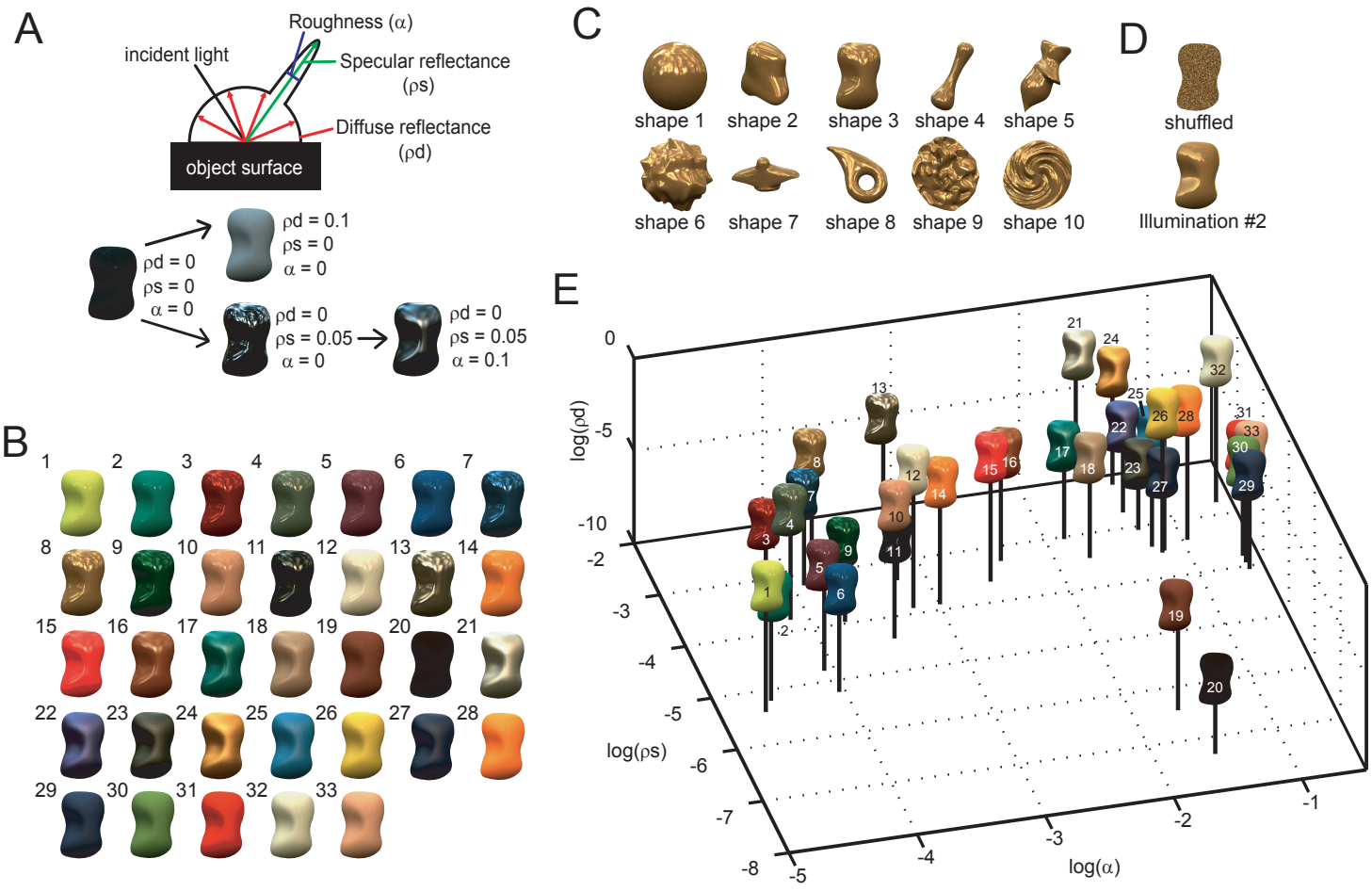
A
Roughness (α)
incident light
Specular reflectance
(ρs)
Diffuse reflectance
(ρd)
object surface
ρd = 0
ρs = 0
α = 0
ρd = 0.1
ρs = 0
α = 0
ρd = 0
ρs = 0.05
α = 0
ρd = 0
ρs = 0.05
α = 0.1
B
C
shape 1
shape 2
shape 3
shape 4
shape 5
shape 6
shape 7
shape 8
shape 9
shape 10
D
shuffled
Illumination #2
E
log(ρd)
log(ρs)
log(α)

Fig. 1

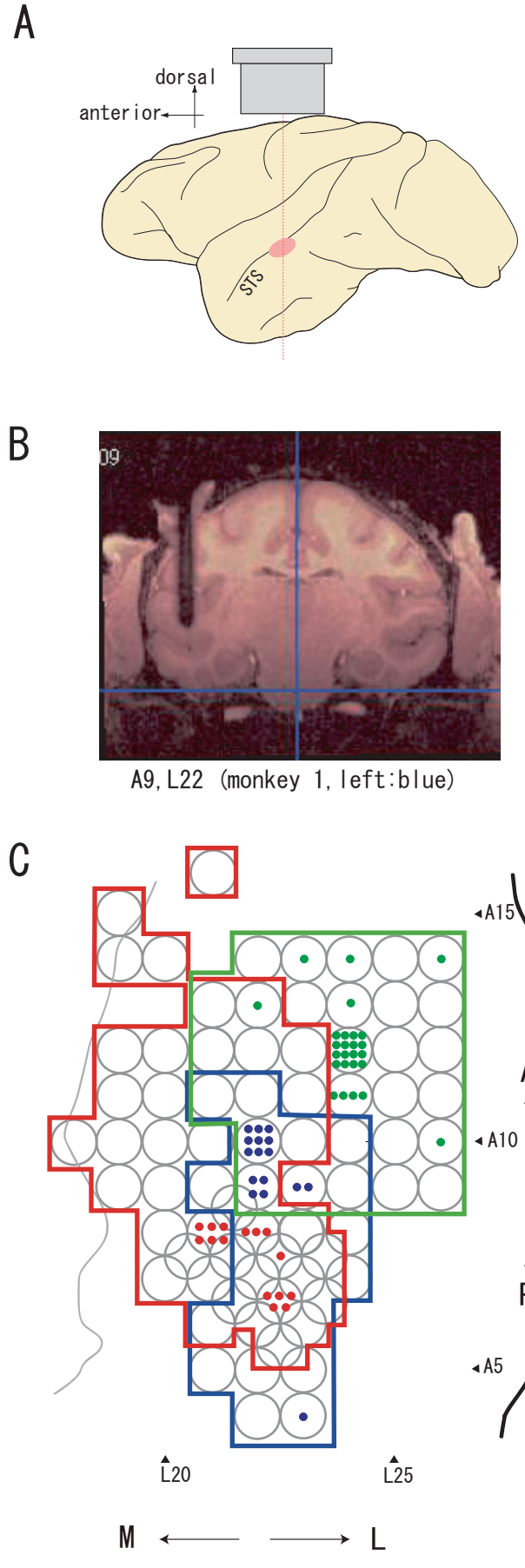
A
dorsal
anterior
STS
B
A9, L22 (monkey 1, left:blue)
C
A15
A
A10
P
A5
L20
L25
M
L

Fig. 2

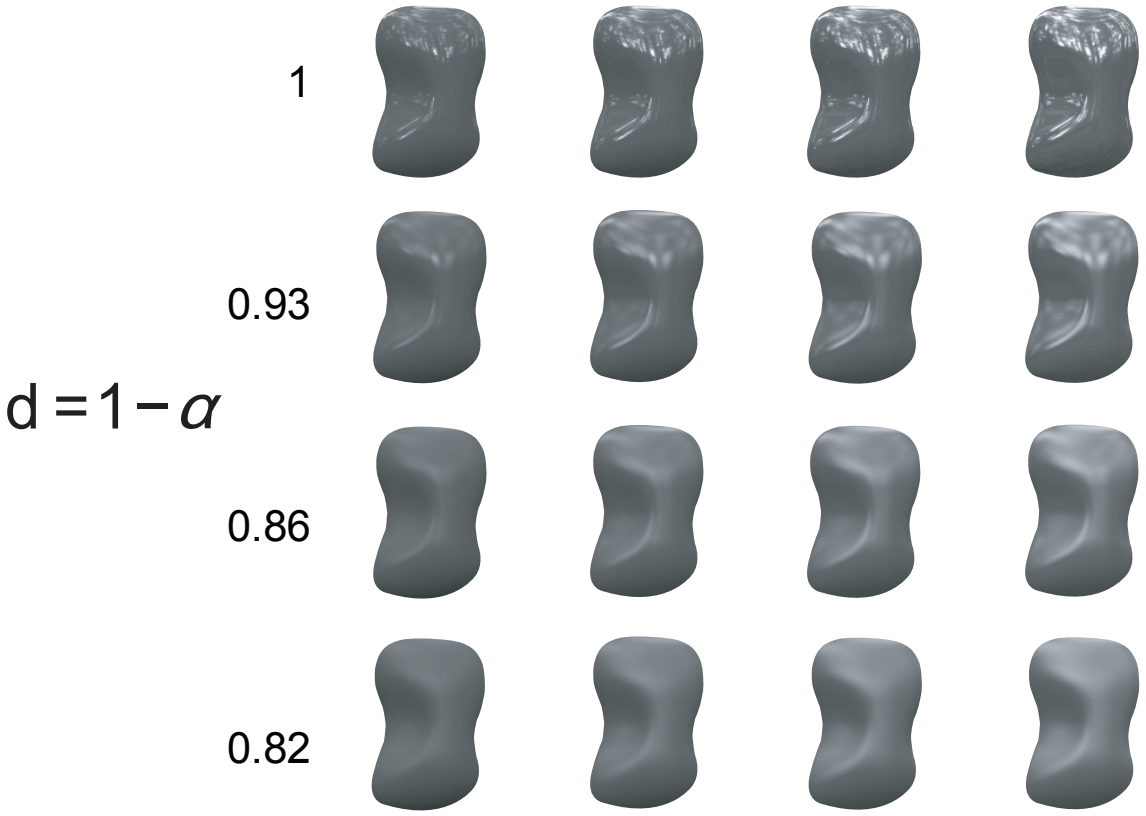

Fig. 3

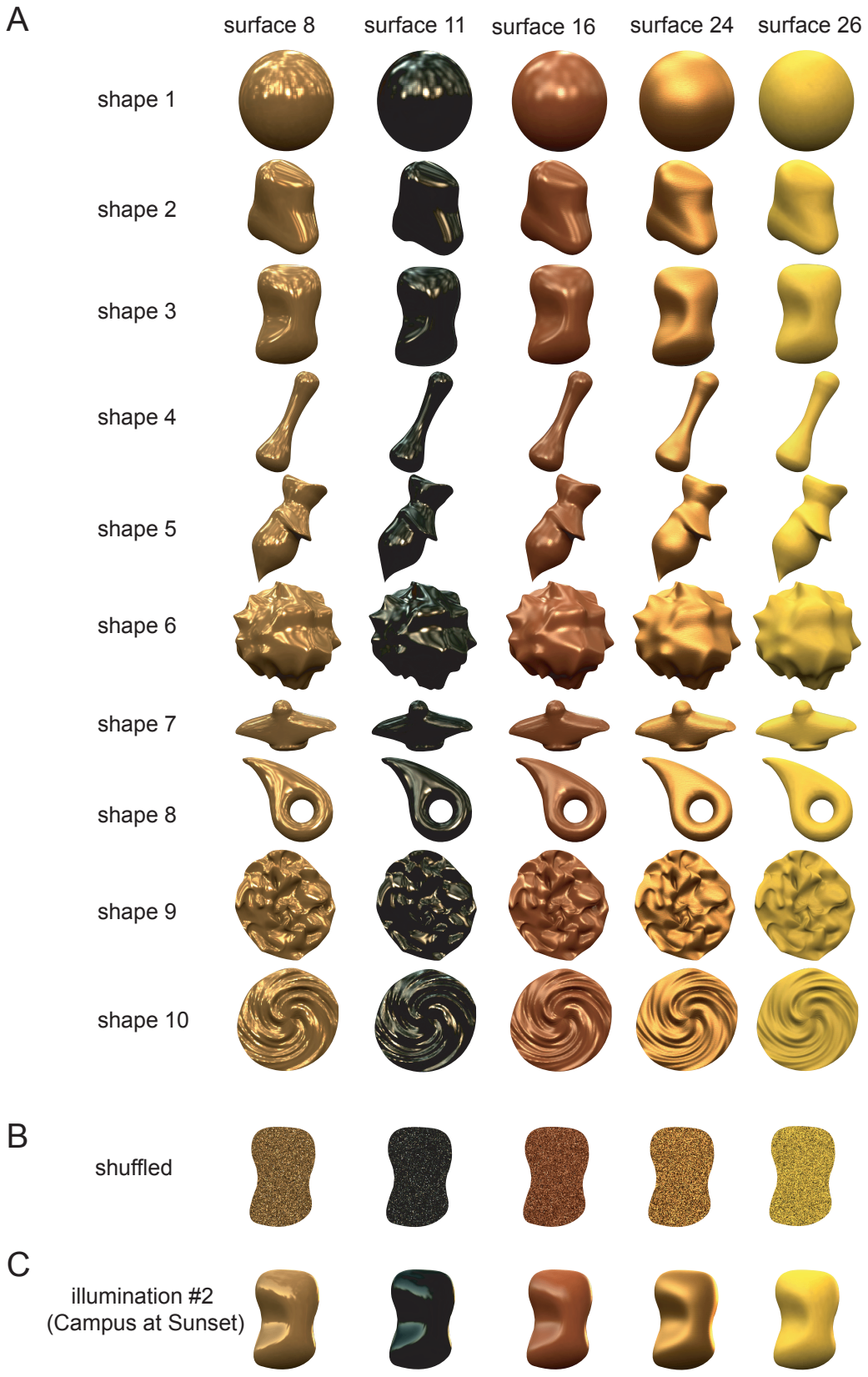
A
surface 8
surface 11
surface 16
surface 24
surface 26
shape 1
shape 2
shape 3
shape 4
shape 5
shape 6
shape 7
shape 8
shape 9
shape 10
B
shuffled
C
illumination #2
(Campus at Sunset)

Fig. 4

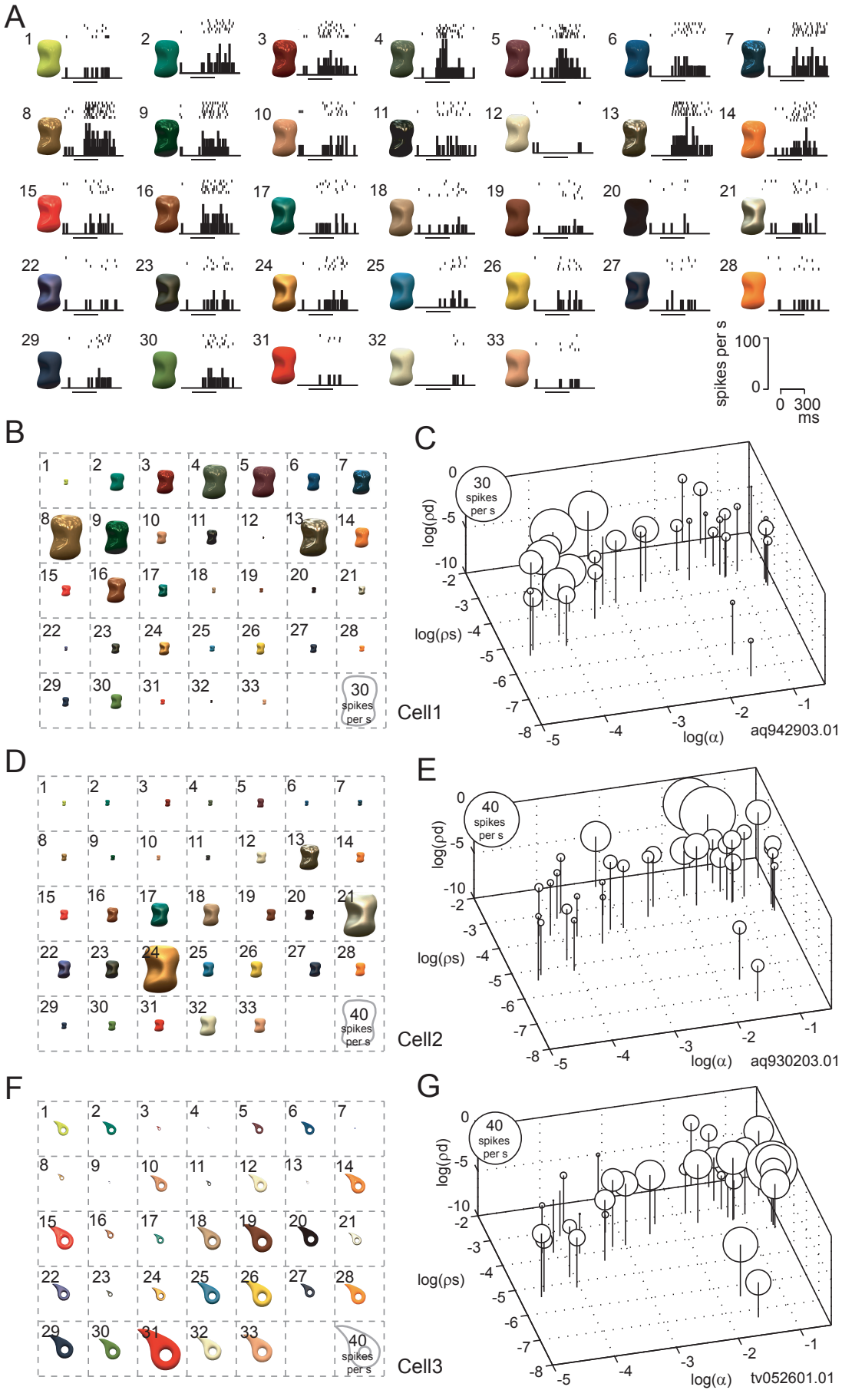
A
spikes per s
100
0
0 300
ms
B
30
spikes
per s
C
Cell1
aq942903.01
log(ρd)
log(ρs)
log(α)
D
40
spikes
per s
E
Cell2
aq930203.01
F
G
Cell3
tv052601.01

Fig. 5

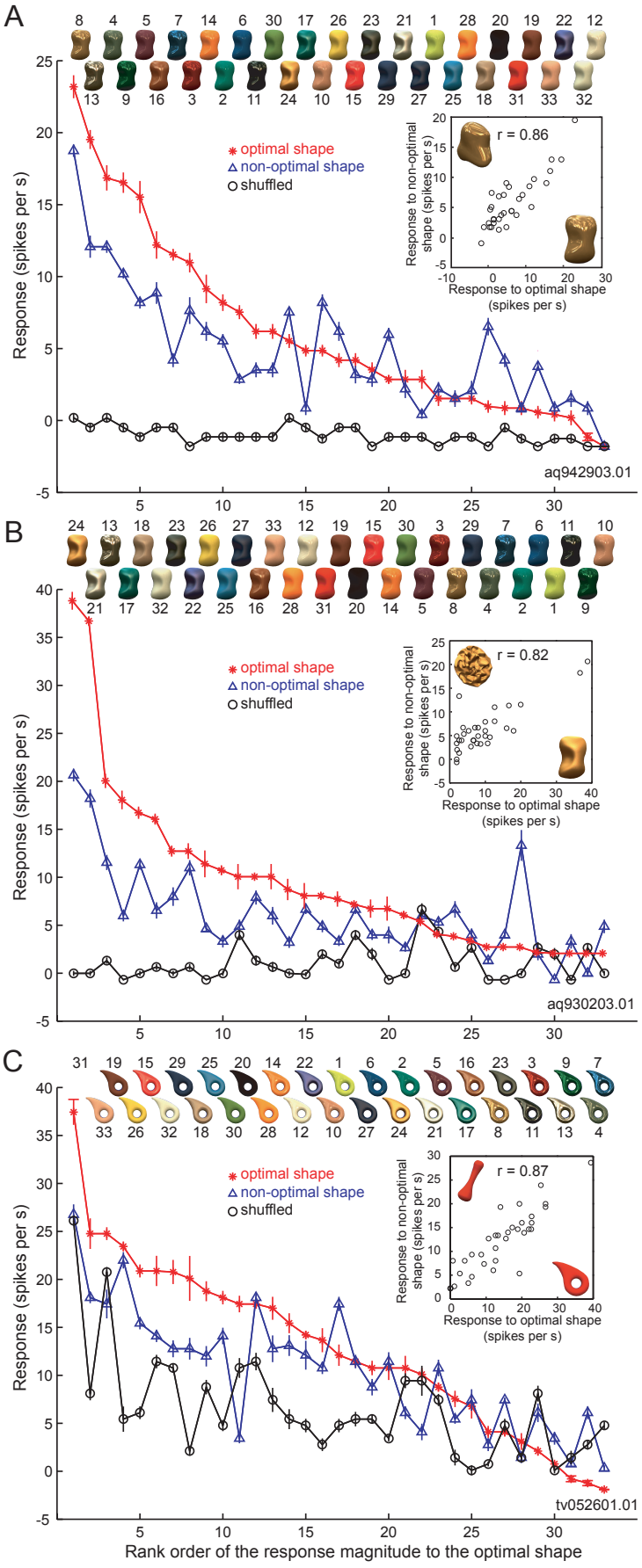
A
8 4 5 7 14 6 30 17 26 23 21 1 28 20 19 22 12
13 9 16 3 2 11 24 10 15 29 27 25 18 31 33 32
optimal shape
non-optimal shape
shuffled
r = 0.86
Response to non-optimal shape (spikes per s)
Response to optimal shape (spikes per s)
Response (spikes per s)
aq942903.01
B
24 13 18 23 26 27 33 12 19 15 30 3 29 7 6 11 10
21 17 32 22 25 16 28 31 20 14 5 8 4 2 1 9
optimal shape
non-optimal shape
shuffled
r = 0.82
Response to non-optimal shape (spikes per s)
Response to optimal shape (spikes per s)
Response (spikes per s)
aq930203.01
C
31 19 15 29 25 20 14 22 1 6 2 5 16 23 3 9 7
33 26 32 18 30 28 12 10 27 24 21 17 8 11 13 4
optimal shape
non-optimal shape
shuffled
r = 0.87
Response to non-optimal shape (spikes per s)
Response to optimal shape (spikes per s)
Response (spikes per s)
tv052601.01
Rank order of the response magnitude to the optimal shape

Fig. 6

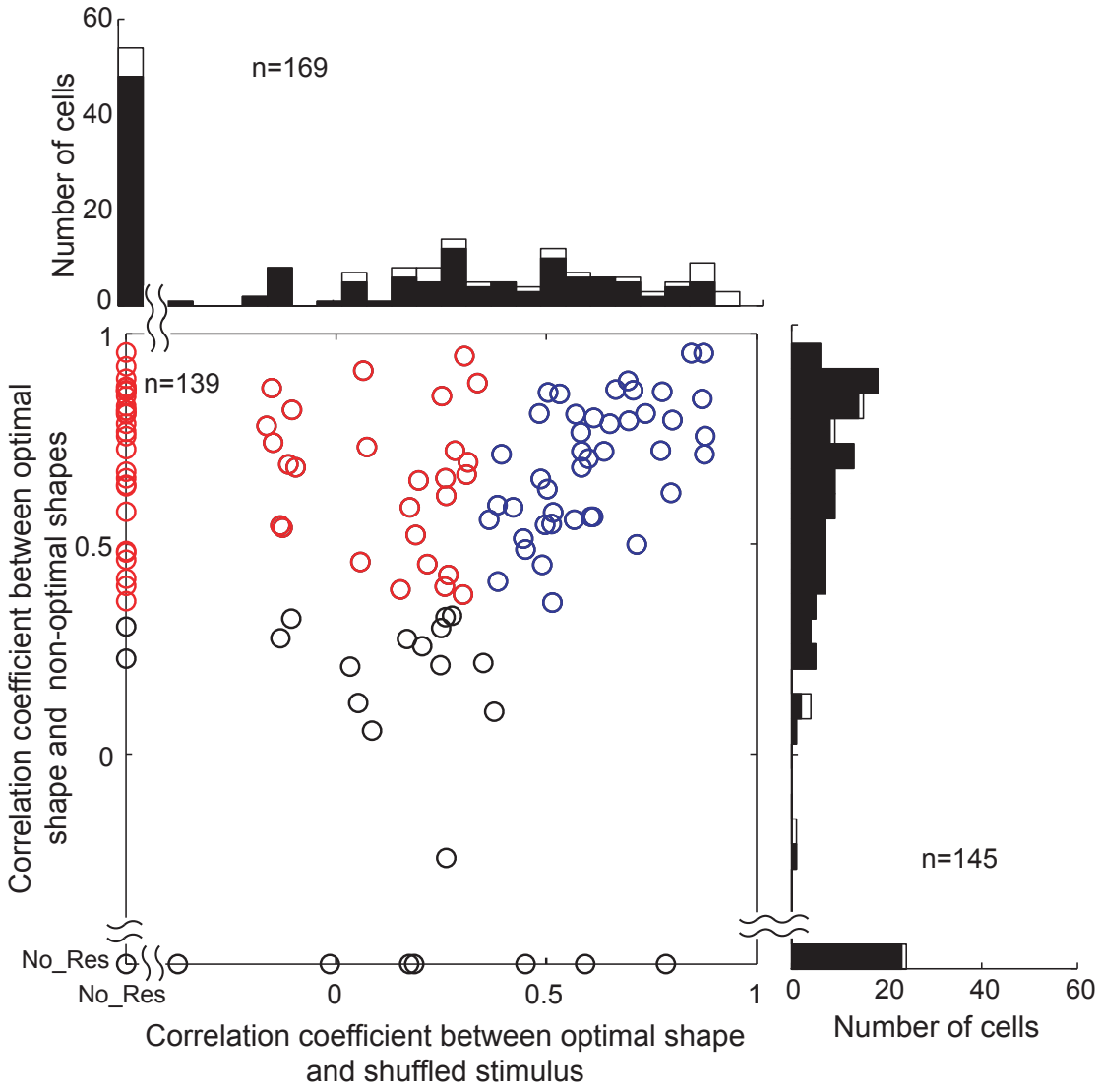
60
40
20
0
Number of cells
n=169
1
0.5
0
n=139
Correlation coefficient between optimal shape and non-optimal shapes
n=145
No_Res
No_Res
0
0.5
1
0
20
40
60
Number of cells
Correlation coefficient between optimal shape and shuffled stimulus

Fig. 7

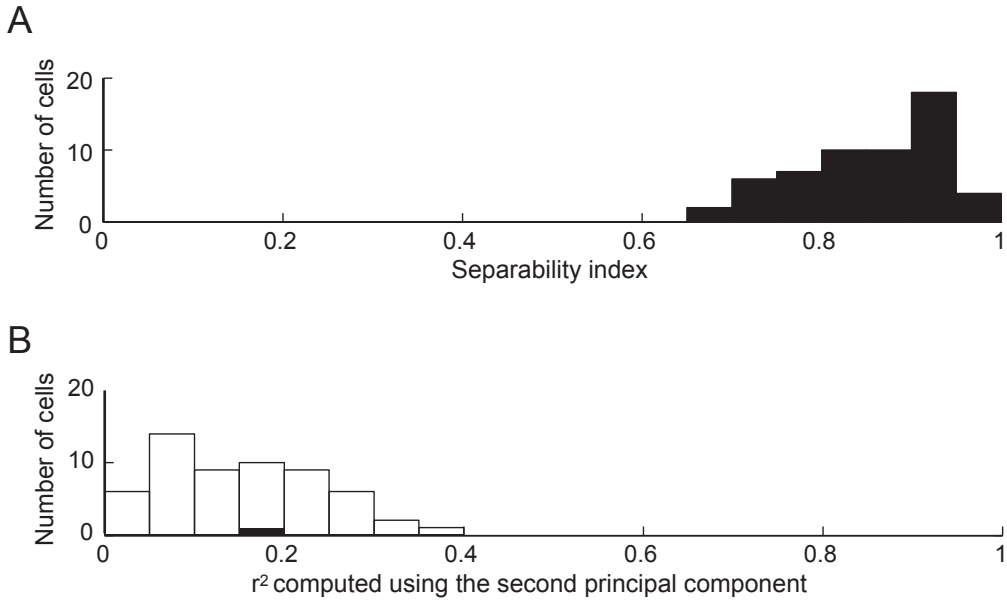
A
Number of cells
20
10
0
0
0.2
0.4
0.6
0.8
1
Separability index
B
Number of cells
20
10
0
0
0.2
0.4
0.6
0.8
1
r2 computed using the second principal component

Fig. 8

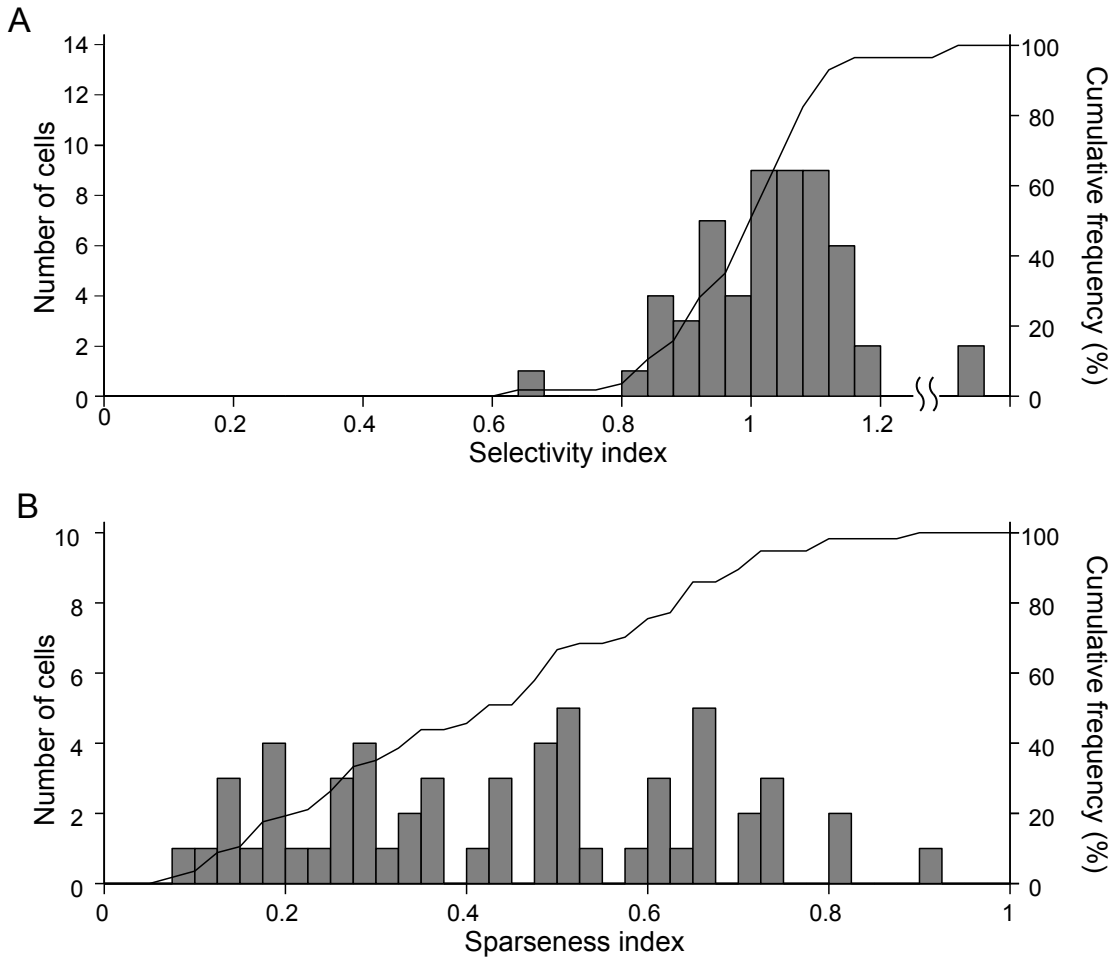
A
Number of cells
Cumulative frequency (%)
Selectivity index
0
0.2
0.4
0.6
0.8
1
1.2
0
2
4
6
8
10
12
14
0
20
40
60
80
100
B
Number of cells
Cumulative frequency (%)
Sparseness index
0
0.2
0.4
0.6
0.8
1
0
2
4
6
8
10
0
20
40
60
80
100

Fig. 9

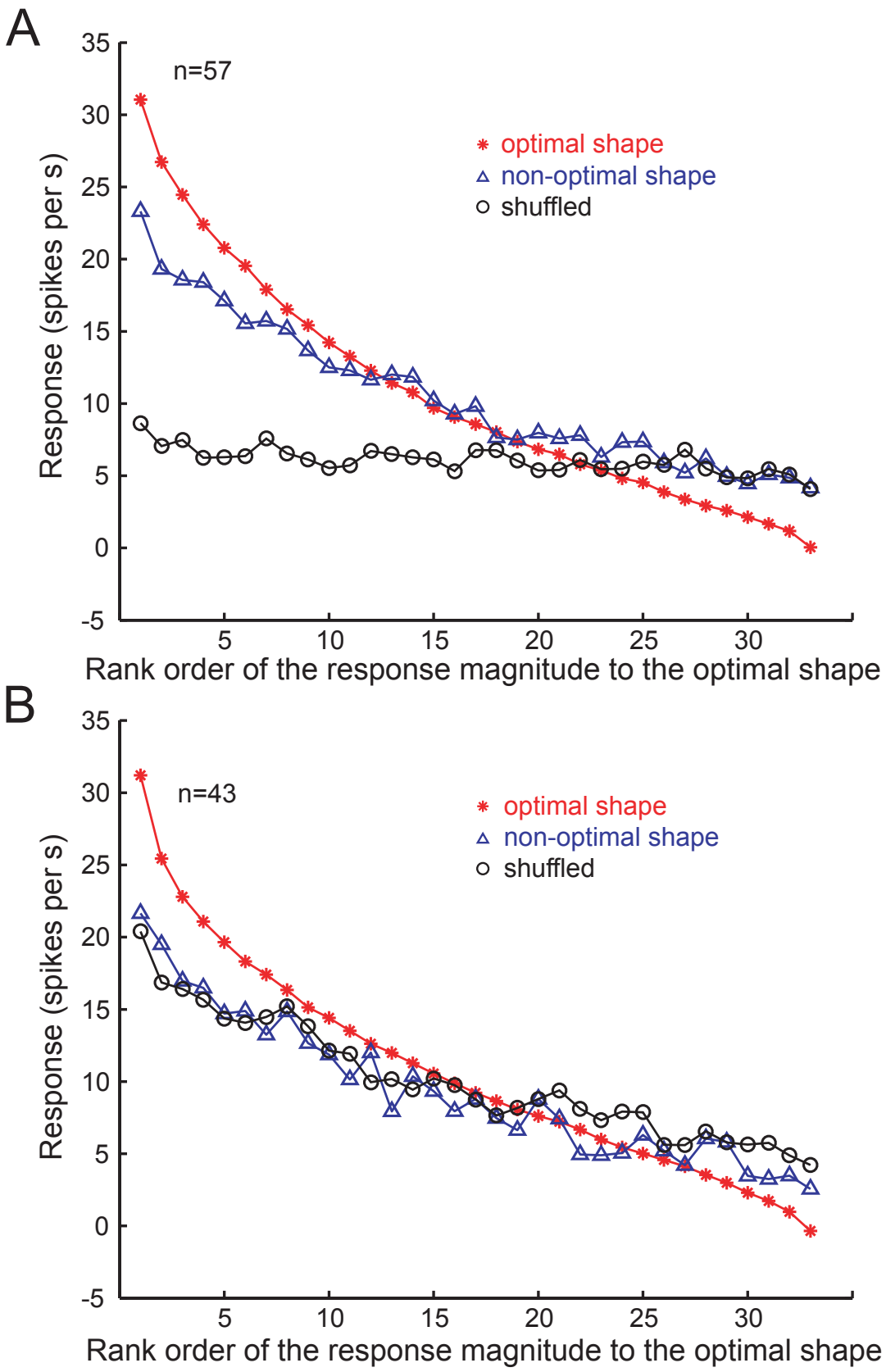
A
n=57
optimal shape
non-optimal shape
shuffled
Response (spikes per s)
35
30
25
20
15
10
5
0
-5
5
10
15
20
25
30
Rank order of the response magnitude to the optimal shape
B
n=43
optimal shape
non-optimal shape
shuffled
Response (spikes per s)
35
30
25
20
15
10
5
0
-5
5
10
15
20
25
30
Rank order of the response magnitude to the optimal shape

Fig. 10

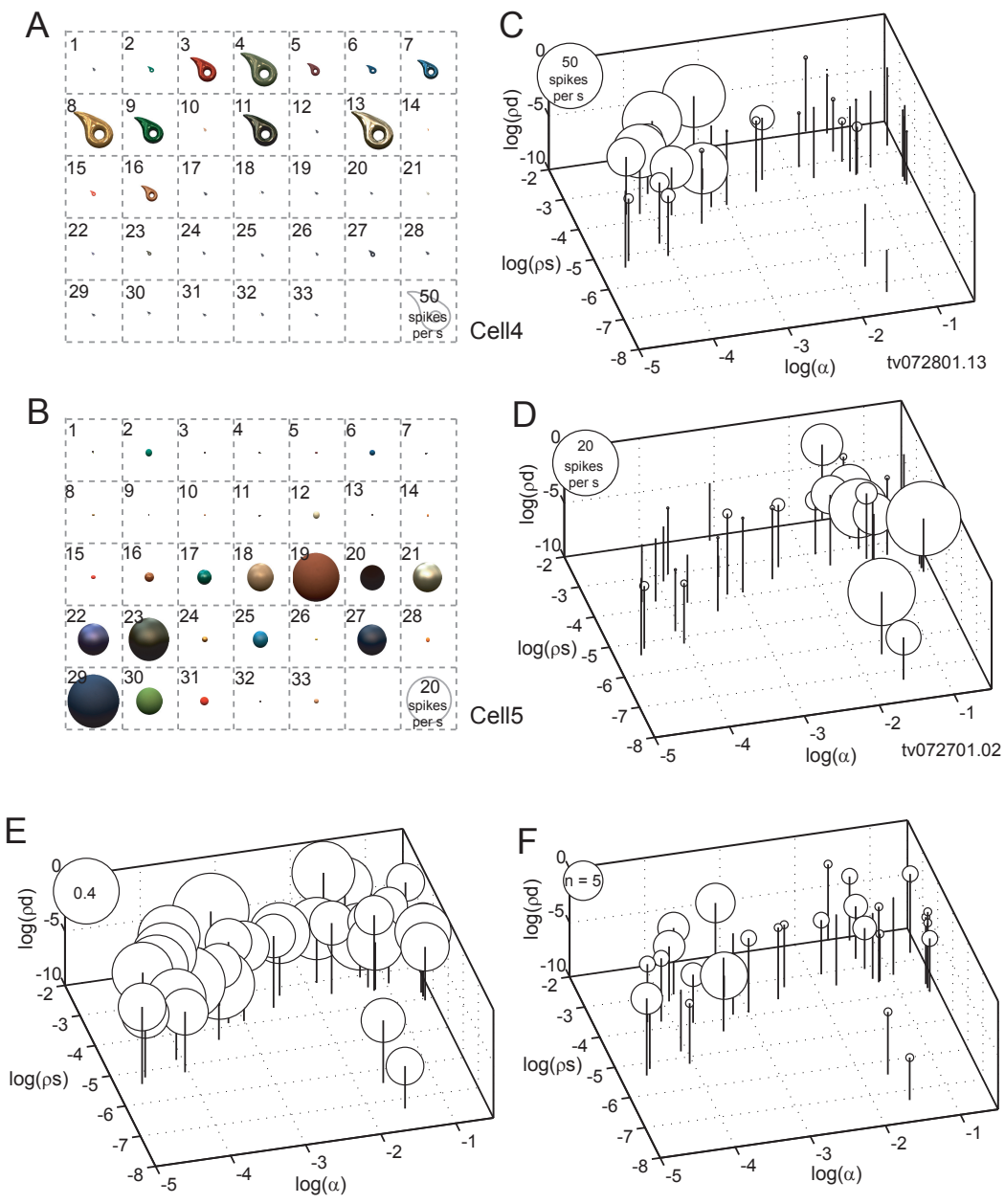
A
1 2 3 4 5 6 7
8 9 10 11 12 13 14
15 16 17 18 19 20 21
22 23 24 25 26 27 28
29 30 31 32 33
50 spikes per s
Cell4
C
50 spikes per s
log(ρd)
log(ρs)
log(α)
tv072801.13
B
1 2 3 4 5 6 7
8 9 10 11 12 13 14
15 16 17 18 19 20 21
22 23 24 25 26 27 28
29 30 31 32 33
20 spikes per s
Cell5
D
20 spikes per s
log(ρd)
log(ρs)
log(α)
tv072701.02
E
0.4
log(ρd)
log(ρs)
log(α)
F
n = 5
log(ρd)
log(ρs)
log(α)

Fig. 11

A

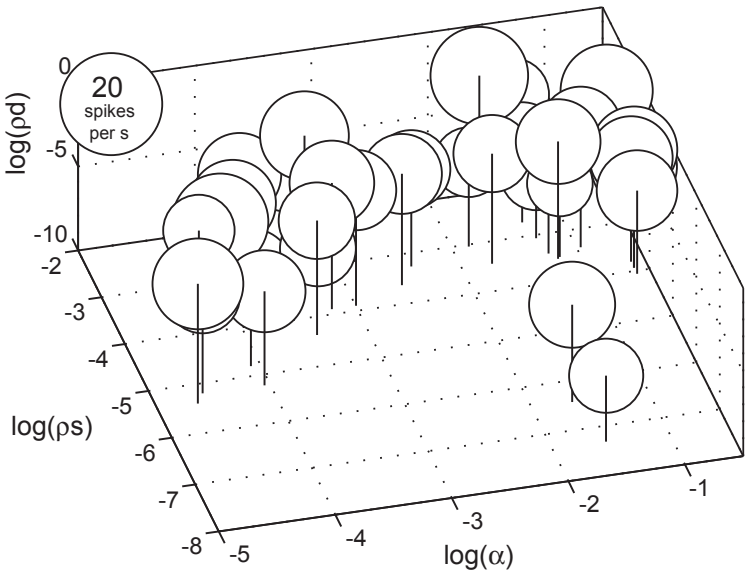
20
spikes
per s
log(ρd)
0
-5
-10
log(ρs)
-2
-3
-4
-5
-6
-7
-8
log(α)
-5
-4
-3
-2
-1

B

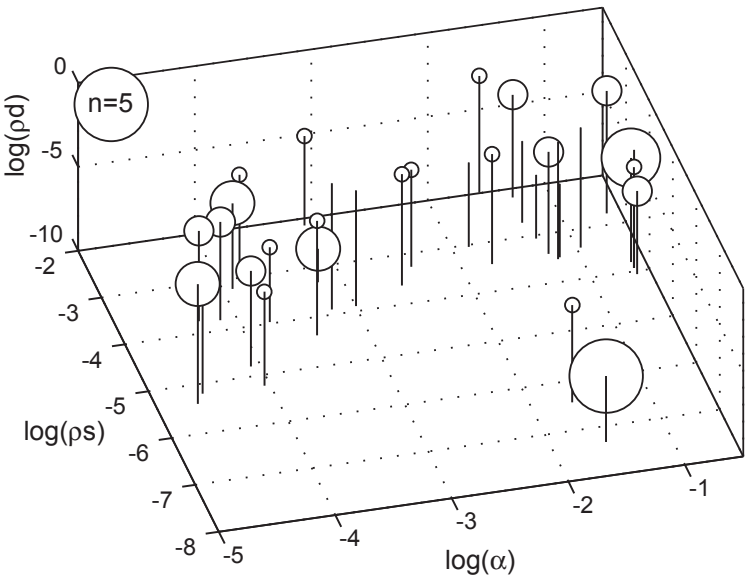
n=5
log(ρd)
0
-5
-10
log(ρs)
-2
-3
-4
-5
-6
-7
-8
log(α)
-5
-4
-3
-2
-1

Fig. 12

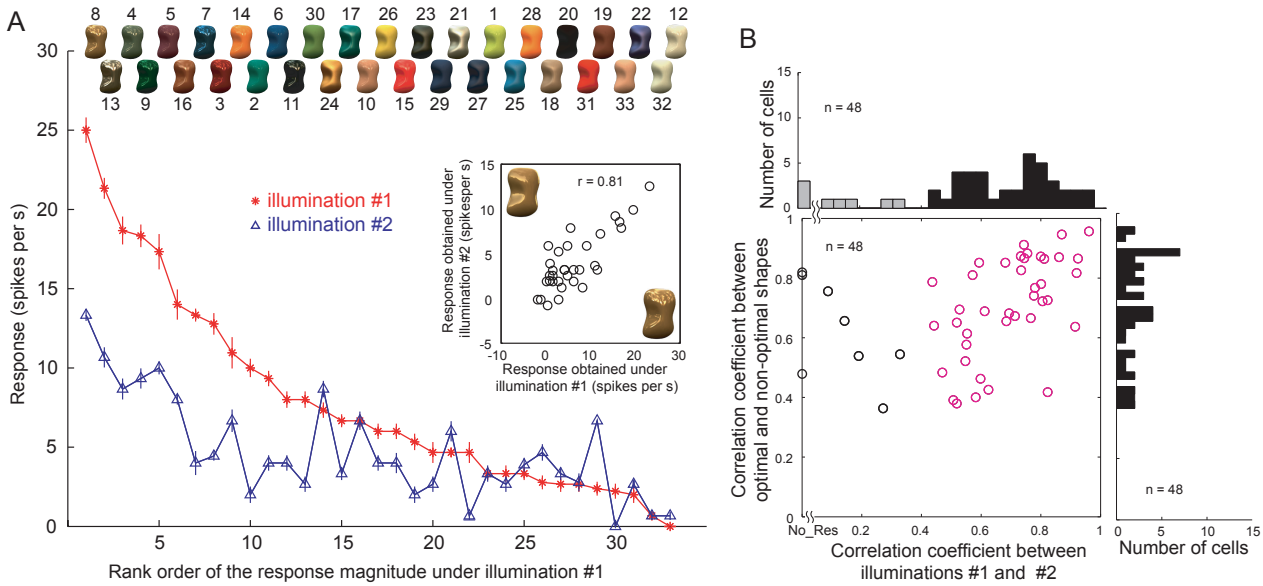
A
8 4 5 7 14 6 30 17 26 23 21 1 28 20 19 22 12
13 9 16 3 2 11 24 10 15 29 27 25 18 31 33 32
Response (spikes per s)
illumination #1
illumination #2
Rank order of the response magnitude under illumination #1
r = 0.81
Response obtained under illumination #2 (spikesper s)
Response obtained under illumination #1 (spikes per s)
B
Number of cells
n = 48
Correlation coefficient between optimal and non-optimal shapes
No_Res
Correlation coefficient between illuminations #1 and #2
Number of cells

Fig. 13

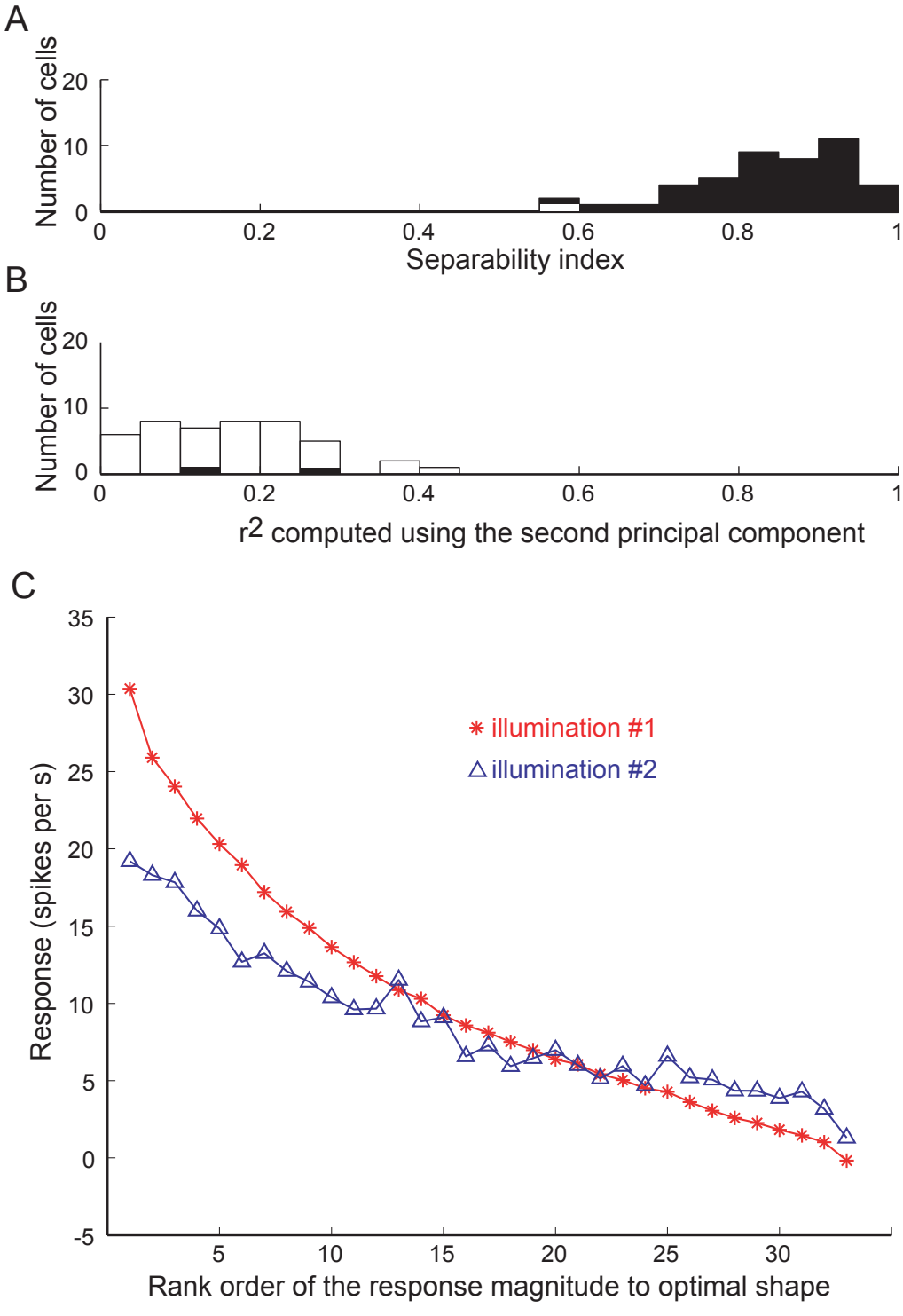
A
Number of cells
20
10
0
0
0.2
0.4
0.6
0.8
1
Separability index
B
Number of cells
20
10
0
0
0.2
0.4
0.6
0.8
1
r2 computed using the second principal component
C
Response (spikes per s)
35
30
25
20
15
10
5
0
-5
5
10
15
20
25
30
illumination #1
illumination #2
Rank order of the response magnitude to optimal shape

Fig. 14

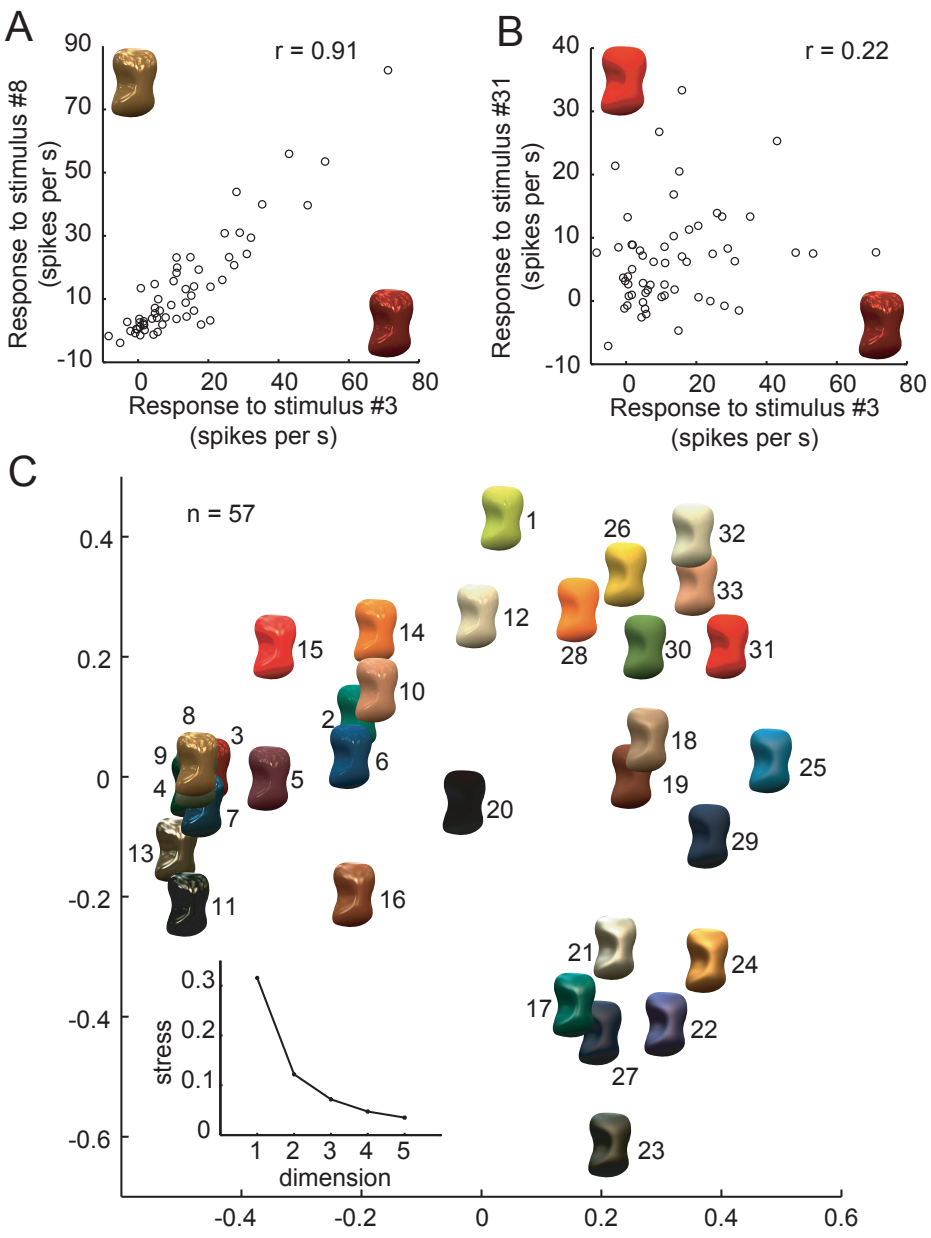
A
r = 0.91
Response to stimulus #8
(spikes per s)
Response to stimulus #3
(spikes per s)
B
r = 0.22
Response to stimulus #31
(spikes per s)
Response to stimulus #3
(spikes per s)
C
n = 57
stress
dimension

Fig. 15

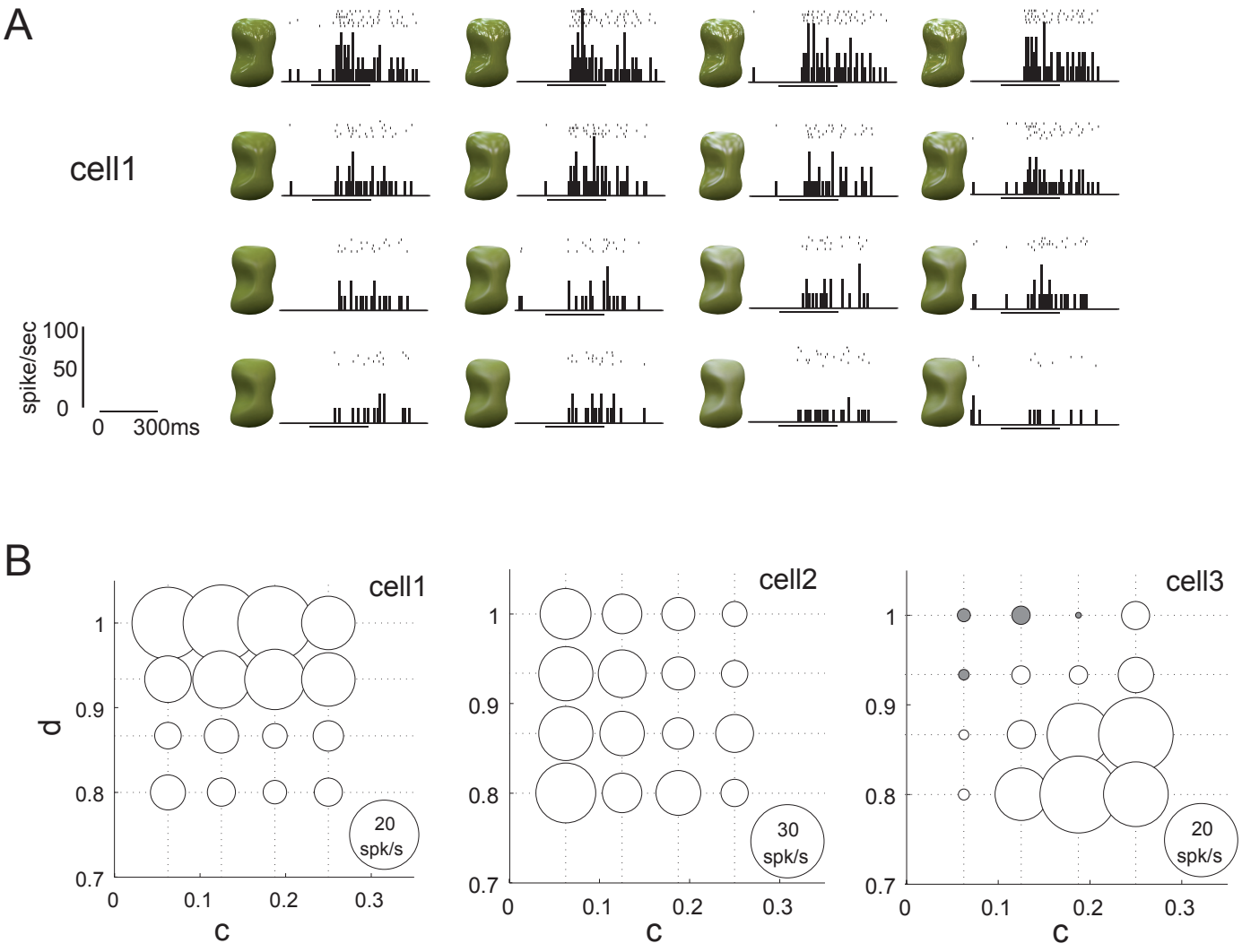
A
cell1
spike/sec
100
50
0
0
300ms
B
cell1
cell2
cell3
d
c
1
0.9
0.8
0.7
0
0.1
0.2
0.3
20
spk/s
30
spk/s
20
spk/s

Fig. 16

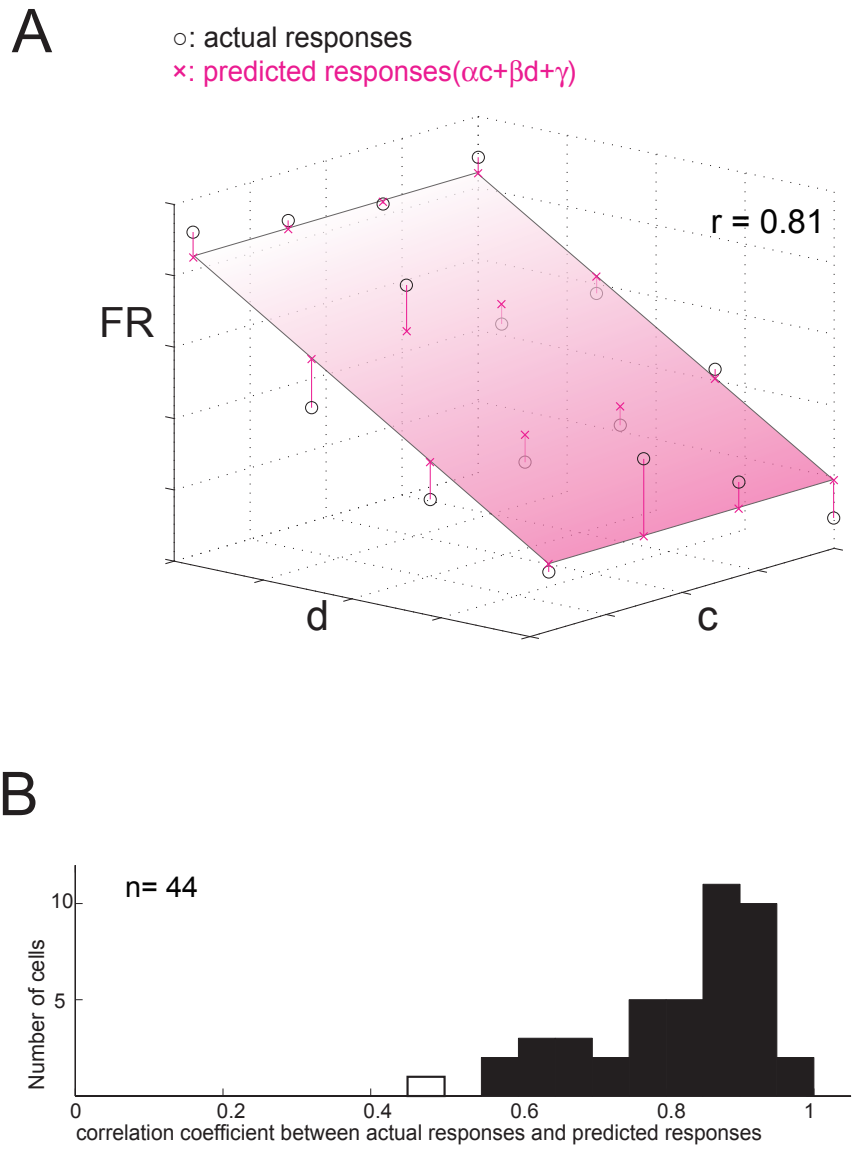
A
○: actual responses
×: predicted responses(αc+βd+γ)
r = 0.81
FR
d
c
B
n= 44
Number of cells
10
5
0
0.2
0.4
0.6
0.8
1
correlation coefficient between actual responses and predicted responses

Fig. 17

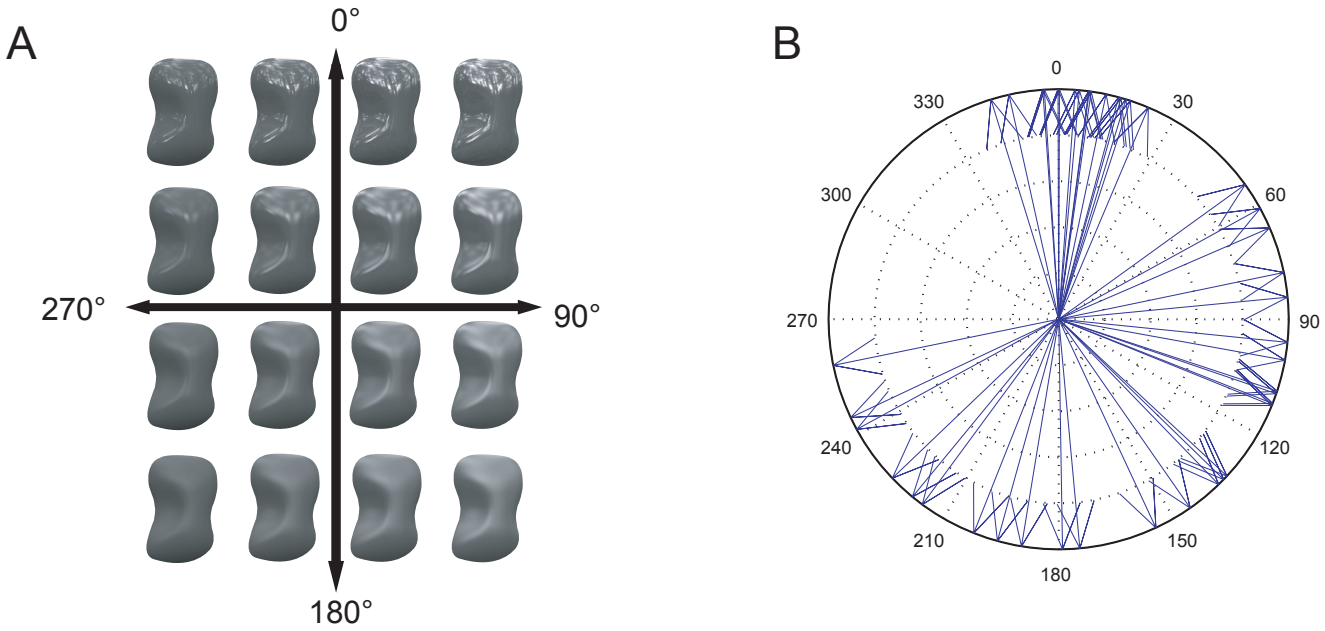

Fig. 18